

AD-A135 077

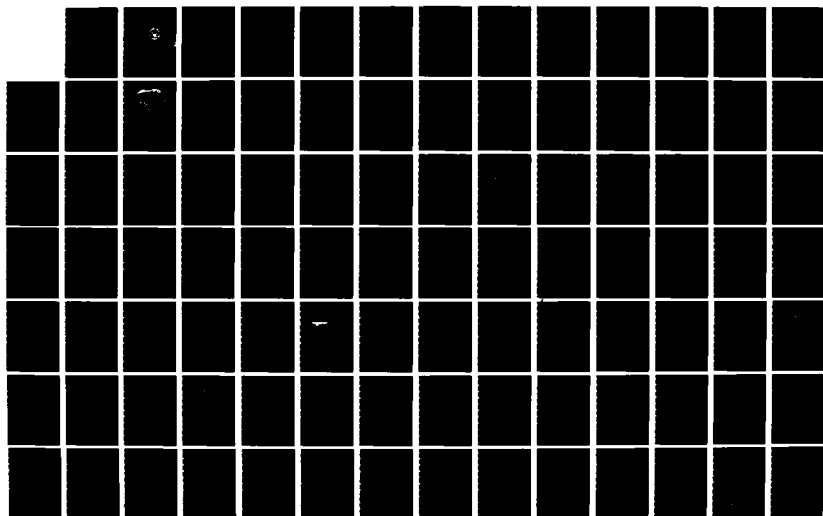
A MODEL FOR TIDAL CIRCULATION ADAPTED TO MONTEREY BAY
CALIFORNIA(U) NAVAL POSTGRADUATE SCHOOL MONTEREY CA
C W SCHOMAKER SEP 83

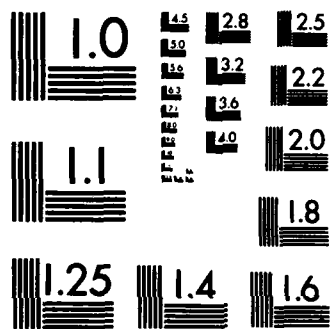
1/2

UNCLASSIFIED

F/G 8/3

NL





MICROCOPY RESOLUTION TEST CHART
NATIONAL BUREAU OF STANDARDS-1963-A

2

NAVAL POSTGRADUATE SCHOOL Monterey, California



DTIC
NOV 29 1983
A

THESIS

A MODEL FOR TIDAL CIRCULATION
ADAPTED TO MONTEREY BAY, CALIFORNIA

by

Christine W. Schomaker

September 1983

Thesis Advisors:

W. E. Hart
E. B. Thornton

Approved for public release; distribution unlimited

DTIC FILE COPY

AD-A133077

83 11 29 021

REPORT DOCUMENTATION PAGE		READ INSTRUCTIONS BEFORE COMPLETING FORM
1. REPORT NUMBER	2. GOVT ACCESSION NO.	3. RECIPIENT'S CATALOG NUMBER
4. TITLE (and Subtitle) A Model for Tidal Circulation Adapted to Monterey Bay, California		5. TYPE OF REPORT & PERIOD COVERED Master's Thesis September 1983
		6. PERFORMING ORG. REPORT NUMBER
7. AUTHOR(s) Christine W. Schomaker		8. CONTRACT OR GRANT NUMBER(s)
9. PERFORMING ORGANIZATION NAME AND ADDRESS Naval Postgraduate School Monterey, California 93943		10. PROGRAM ELEMENT, PROJECT, TASK AREA & WORK UNIT NUMBERS
11. CONTROLLING OFFICE NAME AND ADDRESS Naval Postgraduate School Monterey, California 93943		12. REPORT DATE September 1983
		13. NUMBER OF PAGES 99
14. MONITORING AGENCY NAME & ADDRESS (if different from Controlling Office)		15. SECURITY CLASS. (of this report)
		15a. DECLASSIFICATION/DOWNGRADING SCHEDULE
16. DISTRIBUTION STATEMENT (of this Report) Approved for public release, distribution unlimited.		
17. DISTRIBUTION STATEMENT (of the abstract entered in Block 20, if different from Report)		
18. SUPPLEMENTARY NOTES		
19. KEY WORDS (Continue on reverse side if necessary and identify by block number) Hydrodynamic Model Tide Correctors Tidal Model Hydrographic Survey Monterey Bay Tidal Circulation		
20. ABSTRACT (Continue on reverse side if necessary and identify by block number) An implicit numerical model for two-dimensional hydrodynamic flow in coastal seas by Leendertse (1967), as modified by Hart (1976), was applied to Monterey Bay. The model was tested against available water-level and current observations. The responses of Monterey Bay to tidal forcing and steady-state winds were simulated. Under tidal forcing it was found to provide reasonable estimates of sea-surface elevations. Currents were not well predicted, indicating that other mechanisms such as wind, density stratification, and oceanic currents generally dominate the forcing of the circulation in		

Block 20 cont'd.

Monterey Bay. The model in its present form was found to be potentially suitable for providing real-time tide correctors during a hydrographic survey, achieving an RMS error of 4.5 cm in predicting sea-surface elevations.

Approved For	<input checked="" type="checkbox"/>
Reviewed	<input type="checkbox"/>
Inspected	<input type="checkbox"/>
Released	<input type="checkbox"/>
Classified	<input type="checkbox"/>
Declassified	<input type="checkbox"/>
Excluded	<input type="checkbox"/>
Other	<input type="checkbox"/>

A-1



Approved for public release; distribution unlimited.

A Model for Tidal Circulation
Adapted to Monterey Bay, California

by

Christine W. Schomaker
Lieutenant, NJAA
Sc.B., Brown University, 1972

Submitted in partial fulfillment of the
requirements for the degree of

MASTER OF SCIENCE IN OCEANOGRAPHY (HYDROGRAPHY)

from the

NAVAL POSTGRADUATE SCHOOL
September 1973

Author:

Christine W. Schomaker

Approved by:

William E. Hart

Thesis Co-advisor

Edward B. Thornton

Thesis Co-advisor

Christopher R. Moore

Chairman, Department of Oceanography

M. J. Dyer

Dean of Science and Engineering

ABSTRACT

An implicit numerical model for two-dimensional hydrodynamic flow in coastal seas by Leendertse (1967), as modified by Hart (1976), was applied to Monterey Bay. The model was tested against available water-level and current observations. The responses of Monterey Bay to tidal forcing and steady-state winds were simulated. Under tidal forcing it was found to provide reasonable estimates of sea-surface elevations. Currents were not well predicted, indicating that other mechanisms such as wind, density stratification, and oceanic currents generally dominate the forcing of the circulation in Monterey Bay. The model in its present form was found to be potentially suitable for providing real-time tide correctors during a hydrographic survey, achieving an RMS error of 4.5 cm in predicting sea-surface elevations.

TABLE OF CONTENTS

I.	INTRODUCTION	10
	A. PURPOSE	10
	B. HISTORY OF THE MODEL	11
	C. CIRCULATION STUDIES OF MONTEREY BAY	12
II.	DESCRIPTION OF THE NUMERICAL MODEL	17
	A. HYDRODYNAMIC THEORY	17
	B. STRUCTURE AND COMPONENTS	21
	1. Computational Scheme	21
	2. Computer Program	23
	C. USE AND ADAPTATION	25
	1. Input Data Requirements	25
	2. Subroutine Modifications	26
	3. Computer Implementation	27
III.	APPLICATION OF THE MODEL TO MONTEREY BAY	29
	A. VALIDITY OF ASSUMPTIONS	29
	B. CONSTANT INPUT	29
	1. Time and Space Dimensions	30
	2. Bathymetry and Datum	34
	3. Bottom Friction	35
	C. TIME-VARYING INPUT	36
	1. Initial Conditions	36
	2. Boundary Tidal Amplitudes	36
	3. Boundary Currents	39
	4. Wind	39
	D. DATA FOR COMPARISON	40
	1. Water-level Observations	41
	2. Current-meter Observations	42

IV.	RESULTS	43
	A. COMPARISON OF MODEL RESULTS WITH OBSERVATIONS	43
	1. Sea-surface Elevation Comparisons	43
	2. Current Comparisons	52
	B. MODELED CIRCULATION OF MONTEREY BAY	53
	1. Tidally Forced Circulation	53
	2. Tidally Forced Circulation with Wind	58
V.	CONCLUSIONS	60
	A. VALIDITY OF THE MODEL	60
	B. HYDROGRAPHIC SURVEY APPLICATIONS	60
	APPENDIX A: TIDAL CONSTITUENTS	64
	APPENDIX B: TIDALLY FORCED SEA-SURFACE ELEVATIONS	66
	APPENDIX C: TIDALLY FORCED CURRENTS	80
	BIBLIOGRAPHY	94
	INITIAL DISTRIBUTION LIST	97

LIST OF TABLES

I.	Components of the Numerical Model	24
II.	Comparison of Pelagic and Coastal Tidal Constituents	38
III.	Effect of Various Manning Factors	44
IV.	Effect of Boundary Amplitude Phasing on Grid B . .	52

LIST OF FIGURES

1.1	Map of the Study Area, Showing Model Grids . . .	13
1.2	Bathymetry of Monterey Bay Viewed from Southwest	14
2.1	Staggered Grid of the Numerical Model	22
3.1	Depth Contours for Grid A	31
3.2	Depth Contours for Grid B	32
3.3	Depth Contours for Grid C	33
3.4	Locations of Bathymetric Data in Grid A	34
3.5	Observing Periods for Comparison Data	41
4.1	Sea-surface Elevations at Monterey, Grid A	44
4.2	Elevations at Monterey, $\Delta t=3600$ s	45
4.3	Elevations at Moss Landing, $\Delta t=3600$ s	46
4.4	Elevations at Monterey, $M=.10$ m/s	47
4.5	Elevations at Moss Landing, $M=.10$ m/s	47
4.6	Elevations at Monterey, $\Delta t=900$ s	48
4.7	Elevations at Moss Landing, $\Delta t=900$ s	48
4.8	Spectra, Elevations (SE) at Monterey	49
4.9	Spectra, Elevations (SE) at Moss Landing	50
4.10	Elevations Using Predicted Boundary Amplitudes	51
4.11	Currents near Santa Cruz	54
4.12	Currents South of the Salinas River	55
4.13	Currents North of the Salinas River	56
4.14	Spectra of Currents near Santa Cruz	57
4.15	Current Field for Grid A at 760702 1500	59
5.1	Time Step Lag During Real-time Model	62

ACKNOWLEDGMENTS

The author expresses her appreciation to Drs. Hart and Thornton for their encouragement and guidance. She also thanks Mr. Joe Mullin, Mr. Don Simpson, LT Steve Conrad, and Dr. Terry Hendrix for their help in obtaining digitized field observations. She especially thanks Mr. Eric Schomaker for his unflagging confidence and invaluable editorial assistance.

I. INTRODUCTION

A. PURPOSE

This study grew out of a desire to extend tidal data observed at a few locations to the entire area of a hydrographic survey. With sea-surface elevations modeled over the whole field, survey depths may be corrected automatically by subtracting realistic values of the surface's variation from datum at any point, at any time.

Tidal zoning to obtain sea-surface elevations is, present, a subjective affair requiring numerous water-level stations to indicate the progress of a tidal wave into an inlet. The pattern of propagation at points distant from the observing stations is inferred only qualitatively from bathymetry. Correctors are determined by defining zones graphically and computing appropriate phase and amplitude adjustments for each zone to apply to tidal values observed at the reference stations. This process does not provide a continuum of correctors. It requires subjective judgment and considerable experience to achieve adequate results. The analysis is typically performed well after the survey, when it is too late to use depth data corrected for observed tides to provide cross-checks on the positional accuracy of the data. Errors that might have been detected and corrected during the survey may pass unnoticed until an expensive return to the survey area or downward classification of the survey is necessary.

Use in the field of a two-dimensional, numerical model for circulation and sea-surface elevation would alleviate these difficulties. Such a model must be simple and flexible if it is to be applied in real or near-real time on

field-type microprocessors. In coastal seas and inlets, it should be able to provide sufficiently accurate surface elevations.

To test this concept, the two-dimensional, hydrodynamic model of Leendertse (1967), as modified by Hart (1976) and during this study, was applied to Monterey Bay. The model had previously been used with some success in shallow coastal seas and estuaries, but not in an area with such a dominant bathymetric feature as the Monterey canyon. Although no attempt was made to compare this model to any of the broad spectrum of models in use throughout the oceanographic and coastal-engineering communities [Tracor, Inc., 1971], its relative simplicity, ease of implementation, flexibility, and accurate output are all important to its potential usefulness as a tidal zoning system during field operations.

An additional purpose of this study is to incorporate large-scale non-tidal forces into the model to explore their effects on the circulation and sea-surface elevation of a coastal body of water. Various investigators have suggested, in fact, that tidal forces are overridden in their effect on the circulation of Monterey Bay by the influence of offshore currents and atmospheric conditions. The potential significance of such factors, and the ability to incorporate real-time observations of them into the model, are also important to the model's usefulness as a tidal zoning system.

B. HISTORY OF THE MODEL

The original version of the numerical model used during this study was described by Leendertse (1967). His "multioperational" finite-difference scheme, using both implicit and explicit techniques to solve the equations of

fluid motion, provided advantages in computational stability and efficiency over the explicit models then current [Hart, 1976]. In particular, the model remains stable regardless of the time step used; in a relatively deep embayment such as Monterey Bay the investigator is not restricted to time steps of the order of seconds as is common with explicit models such as that used by Lazanoff (1971) in his study of the bay.

The model has been widely applied, both in small harbors [Leendertse, 1967; Leendertse and Lu, 1975; Chiang and Lee, 1982] and in coastal seas [Leendertse, 1967; Hart, 1976; Spaulding and Beauchamp, 1983]. In past applications, length scales ranged to 290 km and depths ranged to 100 m. This study extends the model to a much deeper area with pronounced vertical relief.

C. CIRCULATION STUDIES OF MONTEREY BAY

Monterey Bay is a relatively large (16 by 42 km), nearly symmetric embayment on the central coast of California. Its most notable bathymetric feature is the Monterey canyon, which curves into the bay from the southwest, severing the continental shelf. Within the bay proper, depths rise from 750 m at the seaward end of the canyon to an average 55 m on the shelf.

The bay presents to the Pacific Ocean one uninterrupted open boundary, some 36 km long. Consequently, oceanic tides and currents and offshore atmospheric effects are primary driving forces of circulation within the bay itself. Local winds and seasonal river runoff may have some effects, especially in the shallower portions of the bay to the north and south. The relative importance of these various influences is not well-understood.

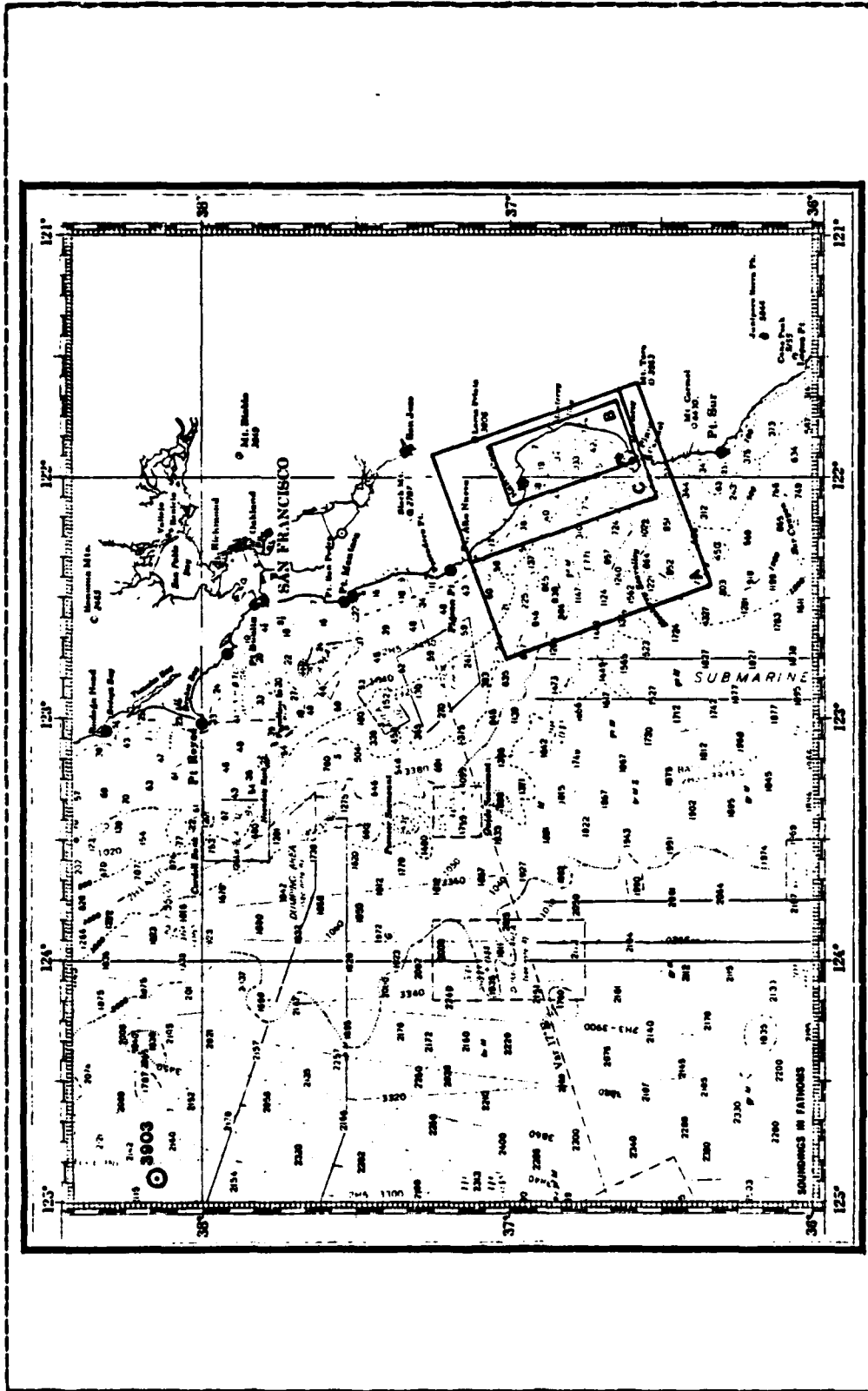


Figure 1.1 Map of the Study Area, Showing Model Grids.

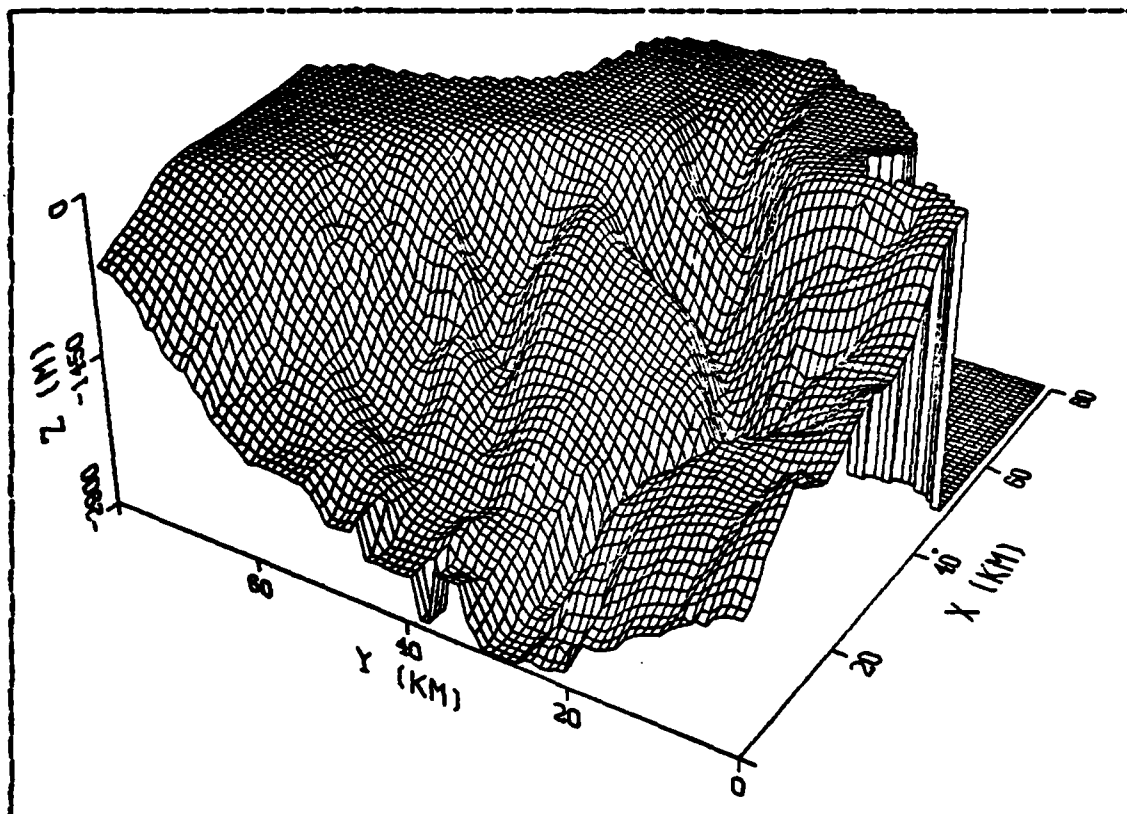


Figure 1.2 Bathymetry of Monterey Bay Viewed from Southwest.

Three oceanographic "seasons" for this portion of the coast were first described by Skogsberg (1936). From November through February the Davidson Current flows northward along the coast in conjunction with southerly or weak northward winds and the onshore transport of surface water. From March through August a period of upwelling is accompanied by the southward flowing California Current, strong northwest winds, and offshore transport of surface water. In September and October the oceanic period is marked by relative calm and an increase in surface temperatures.

All available data concerning circulation within the bay proper were summarized and analyzed in 1973 as part of a major oceanographic study [Scott, 1973]. Normal circulation

was found to be northward through the bay, with a small gyre forming in the southern bight. A more recent analysis by Broenkow and Smethie (1978) also concluded that flow is generally northward, with water entering primarily along the axis of the canyon and having a residence time of 2 to 14 days during upwelling periods. They also suggest that a volume of 10^9 m³ pumped into and out of the bay by internal tidal mixing may be responsible for the frequent presence of cool, nutrient-rich waters at the head of the Monterey Canyon near Moss Landing.

Most circulation studies of the bay proper have relied primarily on temperature and salinity data collected at oceanographic stations. Although drift cards and similar devices have been used to map surface currents, long-term current-meter observations have not been available until the last ten years. During predesign studies for sewer outfalls, current meters were deployed for periods of a year or more near Santa Cruz [Brown and Caldwell, Inc., 1978], the Pajaro River [Environmental Research Consultants, Inc., 1976], and the Salinas River [Engineering-Science, Inc., 1977]. In general, these studies suggest that the net flow of water is northward along the coast, with some dependence on the local diurnal wind.

Tidal forcing has not been examined closely in any of the aforementioned studies. However, an explicit numerical model was employed by Lazanoff (1971) to study the tidal circulation within the bay. Although field observations indicated that the primary driving force for circulation derived from oceanic currents, the tide- and wind-driven model did predict correct sea-surface elevations and current phases and directions for the short time periods over which it could be run. Current magnitudes appeared too large near coastal boundaries.

More recently Bretschneider (1980) analyzed the effects of various oceanographic conditions on the sea-level changes observed at Monterey. Variations in geostrophic current flow, atmospheric pressure, sea-surface temperature, and meridional wind stress were shown to correspond to observed variations in sea-surface elevation at Monterey.

II. DESCRIPTION OF THE NUMERICAL MODEL

A. HYDRODYNAMIC THEORY

The numerical model of Leendertse (1967) relies on the basic equations that describe conservation of momentum and mass for incompressible fluid motion. In the Cartesian coordinate system of the model, with x- and y-axes embedded in a horizontal f-plane tangent at the origin to the undisturbed sea surface (the datum) and with the z-axis oriented upward, these well-known equations are:

$$\frac{\delta u}{\delta t} + u \frac{\delta u}{\delta x} + v \frac{\delta u}{\delta y} + w \frac{\delta u}{\delta z} = -\frac{1}{\rho} \frac{\delta p}{\delta x} + F_x \quad (2.1)$$

$$\frac{\delta v}{\delta t} + u \frac{\delta v}{\delta x} + v \frac{\delta v}{\delta y} + w \frac{\delta v}{\delta z} = \frac{1}{\rho} \frac{\delta p}{\delta z} + F_y \quad (2.2)$$

$$\frac{\delta w}{\delta t} + u \frac{\delta w}{\delta x} + v \frac{\delta w}{\delta y} + w \frac{\delta w}{\delta z} = \frac{1}{\rho} \frac{\delta p}{\delta z} + F_z \quad (2.3)$$

$$\frac{\delta u}{\delta x} + \frac{\delta v}{\delta y} + \frac{\delta w}{\delta z} = 0 \quad (2.4)$$

The variables u , v , and w are components of velocity parallel to the x-, y-, and z-axes respectively, p is pressure, and ρ is density. The applied forces per unit mass (F_i) represent effects of the Earth's rotation, the Earth's gravitation, viscous and turbulent stresses in the fluid, and astronomical tides.

These equations are simplified by making assumptions appropriate to the examination of long-period forcing in a two-dimensional, shallow field. Detailed derivations may be found in Leendertse (1967) and Hart (1976). A more general development of shallow water equations may be found in Csanady (1982). The necessary assumptions are summarized in the following paragraphs.

First, because a coastal sea or estuary is generally shallow relative to the horizontal scale of motion, the vertical velocity is assumed small relative to the horizontal velocities. Therefore, both convective-inertia terms and rotational effects that involve the vertical velocity in equations 2.1-2.3 may be neglected.

Second, the equations 2.1-2.4 are averaged to model fluid motions with periods greater than those of short-period turbulent motions.

Third, the hydrostatic approximation is made by analysis of equation 2.3. The vertical component of the rotational effect may be considered negligible (of the order 10^{-2} cm/s²) and so may vertical stress-gradient effects (10^{-3} cm/s² according to Csanady, 1982). Furthermore, since mean vertical velocities are unlikely to be greater than 10 cm/s, over sufficiently long time periods ($>10^3$ s or 15 minutes) the total vertical acceleration will be of similarly small order. Neglecting for the moment tidal effects, an expression for pressure may be obtained by integrating the remaining terms over depth:

$$p = p_a + g \int_z^{\eta} \rho \delta z \quad (2.5)$$

In this expression, η is the sea-surface elevation and p_a is the atmospheric pressure at the sea surface, both functions of x and y . The gravitational acceleration, g , is assumed constant and equal to its mean value at the undisturbed sea surface.

Equation 2.5 permits computation of pressure gradients, $\delta p/\delta x$ and $\delta p/\delta y$, from horizontal gradients in sea-surface elevation and density. Gradients in atmospheric pressure may be neglected since their effect is small relative to the turbulent stress induced at the surface by the wind. In the numerical model, tidal forcing is accomplished by generating gradients of sea-surface elevation rather than by attempting to simulate directly the astronomical forces that cause the tides.

Fourth, the Boussinesq approximation is made, in which the influence of vertical density variations is assumed to be negligible. For this to be true the area to be modeled must be vertically well-mixed, an assumption that is not generally applicable. Although the version of Leendertse's model used in this study requires this assumption, some compensation for density stratification might be made by modifying the model to integrate estimated values for the vertical density variation over the depth at each point to obtain the additional density-induced sea-surface elevation [Csanady, 1982].

Fifth, the mean viscous-shear stresses of the fluid are assumed negligible, leaving only the turbulent stresses (Reynolds stresses) at boundaries within and external to the fluid to be formulated. Of these, sharp density gradients within the fluid are neglected as a source of stress. Closed lateral boundaries are considered by applying the coastal boundary condition that velocity into the boundary is zero. Two other boundaries are considered, the sea surface and the bottom, and algorithms for modeling stresses on these boundaries must be prepared.

Sixth, since interior stresses resulting from sharp density boundaries are assumed negligible, equations 2.1 and 2.2 may be integrated vertically to provide implicit expressions for horizontal velocities averaged over depth.

Applying the kinematic boundary condition at the free surface and at the bottom (assumed impermeable), equation 2.4 may also be integrated vertically using the Leibnitz rule of integration. Three equations implicit in three unknowns are then available for the vertically integrated, horizontal velocities U and V and the free, sea-surface elevation η :

$$\frac{\delta U}{\delta t} + U \frac{\delta U}{\delta x} + V \frac{\delta U}{\delta y} = -g \frac{\delta \eta}{\delta x} + fV + (F_{Wx} - F_{Bx})/\rho(h+\eta) \quad (2.6)$$

$$\frac{\delta V}{\delta t} + U \frac{\delta V}{\delta x} + V \frac{\delta V}{\delta y} = -g \frac{\delta \eta}{\delta y} - fU + (F_{Wy} - F_{By})/\rho(h+\eta) \quad (2.7)$$

$$\frac{\delta \eta}{\delta t} + \frac{\delta(h+\eta)U}{\delta x} + \frac{\delta(h+\eta)V}{\delta y} = 0 \quad (2.8)$$

In these equations f is the Coriolis parameter, h is the depth, F_{Wi} is the surface friction stress due to wind, and F_{Bi} is the bottom friction stress. U and V are mean horizontal velocities over the water column. This simplification results in a two-dimensional model with which patterns of circulation and sea-surface elevation may be quantitatively determined.

Finally, since bottom stress depends on the fluid velocity, a well-known quadratic model is assumed so that the stress term may be incorporated directly into Leendertse's computational scheme. The formulation for bottom stress is:

$$F_{Bx} = \rho g U (U^2 + V^2)^{1/2} / C^2 \quad (2.9)$$

$$F_{By} = \rho g V (U^2 + V^2)^{1/2} / C^2 \quad (2.10)$$

The empirical Chezy coefficient, C , may be computed in any of various ways and must be specified for the area to be modeled.

B. STRUCTURE AND COMPONENTS

A derivation of the numerical model, a discussion of its computational stability, and a program listing are given by Leendertse (1967). Key features of the computational scheme and the computer program used during this study are presented here.

1. Computational Scheme

In the numerical model, equations 2.6-2.8 are approximated with a finite-differencing scheme extending over two time levels, each a half time step. At the first half time step, $t+1/2$, the velocity $U(t+1/2)$ and the sea-surface elevation $\eta(t+1/2)$ are computed implicitly and the velocity $V(t+1/2)$ is computed explicitly. At the second half time step, $t+1$, the velocity $V(t+1)$ and sea-surface elevation $\eta(t+1)$ are computed implicitly and $U(t+1)$ is computed explicitly.

Computations are spatially controlled by a uniform grid of squares laid over the f -plane (Figure 2.1). Depths relative to the undisturbed sea surface, here taken to be mean lower low water (MLLW), must be supplied for the corners of each square, values of horizontal velocity are computed at the centers of the sides of each square, and values of sea-surface elevation are computed at the center of each square. Wind-stress and bottom-friction factors must be specified or computed at the centers of each square. This staggered-grid is basic to the spatial realization of

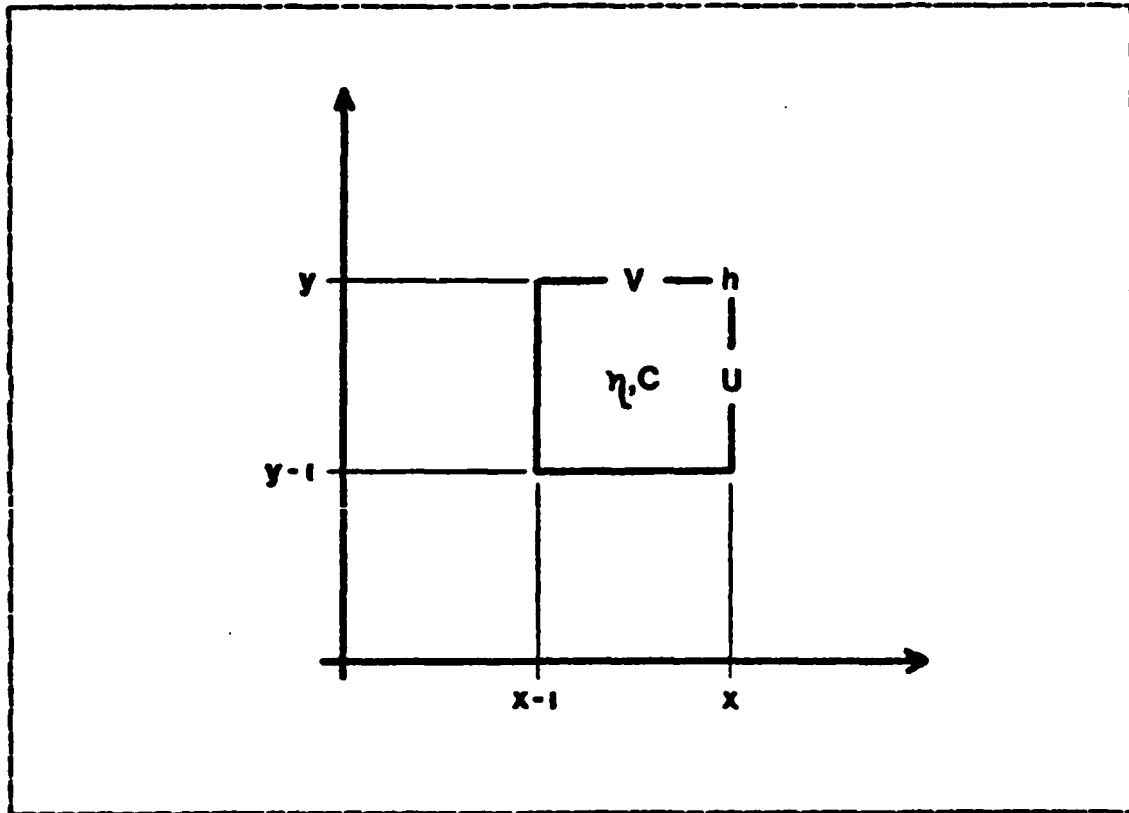


Figure 2.1 Staggered Grid of the Numerical Model.

Leendertse's finite-differencing scheme in that the mean velocity into or out of each square is used to compute the change in sea level within. The grid also permits the coastal constraint of zero transport perpendicular to sea/land boundaries.

During the first half time step, implicit computations proceed row by row from left to right and explicit computations proceed column by column from the bottom to the top of the grid. During the second half time step this process is reversed, "centering" the results in space as well as time.

2. Computer Program

The computer program used to model Monterey Bay is a modified version of a Fortran program developed by Hart (1976). It includes provisions for modeling wind stress, steady flow at boundary points, and overflow at boundary points, none of which were available in Leendertse's original listing. To increase the flexibility of the program, additional modifications have been made during this study. These include:

- Introduction of date and time computations to permit the program to search time-coded files for data items required at each half time step.
- Direct computation of bottom-friction factors from an average bottom-type parameter or from a grid of bottom types.
- Creation of an interactive subroutine to start the program by prompting the user for parameters critical to each run.
- Output of time series of currents and sea-surface elevation for up to nine points in the model grid.
- Further modularization of the model's functional components.

The core of the program is subroutine MODEL, which contains the finite-differencing scheme of Leendertse. Other subroutines serve auxiliary functions: Interactively starting the run, acquiring both constant and time-dependent data, specifying conditions at boundary points, specifying numerical models for wind and bottom stress, and supplying

results in various output formats. An outline of the program is presented in Table I.

TABLE I
Components of the Numerical Model

MAKEGRID	Generate depth and computation-control grids.
BAYMODEL	Main program to control each run of the model.
START	Interactively input run-time parameters.
DIMENS	Input constant data for grid of area.
FIND	Locate water sections to be modeled.
INVAL	Initialize variables everywhere in grid.
INCURR	Initialize currents as desired.
MODEL	Multioperational finite-difference scheme.
CHEZY	Supply Chezy coefficient at each grid point.
WIND	Supply wind stress term at each grid point.
RESULT	Compute output values in desired units.
OPEN	Specify sea-surface elevations at open bounds.
STEADY	Specify currents at open bounds and rivers.
OVFLO	Specify overflow currents at boundaries.
OVFLD	Specify overflow thresholds.
INTIDE	Set tide from a time-coded file.
INWIND	Set wind from a time-coded file.
HEADS	Output headers for each output file.
PRINT	Output results for desired times.
PLOT	Output results needed for graphic display.
SERIES	Output results for specific points.
PTGRID	Utility print of input gridded data.
CALEND	Utility for number of days in month.
ADTIME	Utility to increment time.
BAYPLOT	Provide graphic presentation of results
ELEVCOMP	Compare elevation series with observed data.
CURRCOMP	Compare current series with observed data.

Some subroutines, such as OPEN, must be prepared specifically for the area to which the model is applied, while others, such as MODEL, should not be altered. Modularization of the program permits the user to readily

change the appropriate functions when adapting the model to different coastal areas (and computers).

C. USE AND ADAPTATION

When applying the numerical model to a specific area, certain requirements concerning input data and program modification must be met. These are discussed below.

1. Input Data Requirements

Each run of the numerical model requires specification of start and end times, time-step length, and an interval at which results must be output. For experimental (as opposed to operational) use, other things may be specified: Points at which series output is desired, the type of output, and omission of certain terms in the hydrodynamic equations.

Input values that are unique to the area to be modeled and that do not change from one run to the next must also be supplied. These values are most conveniently stored in a separate file. They include:

- A location title and central latitude.
- Dimensions of the grid.
- Depths for each grid corner.
- Control numbers for each grid square (land=0, water=1, overflow=2).
- A general bottom-friction parameter or a bottom-type indicator for the center of each grid square.
- Number of tide stations supplying data for boundary conditions.
- Number of wind stations supplying data.

Selection of the size of grid to be used is limited by the size of the area to be modeled and the available virtual memory and CPU time of the computer. Since depths, friction and wind factors, output data, and two half-time-step values for each velocity component and the sea surface elevation must be available for each grid square at all times, at least 12 arrays must be dimensioned according to the grid size and survey area. The maximum dimensions of 80 by 80 used in this study required close to 1 megabyte of virtual computer memory and approximately 0.5 s of CPU time per time step on the IBM 3033 mainframe computer.

2. Subroutine Modifications

Stresses at the bottom and surface must be modeled in the subroutines CHEZY and WIND. Since Leendertse's model already assumes a quadratic formulation for bottom friction, only the Chezy factor, C, need be provided by the subroutine CHEZY; however, many empirical techniques exist for computing the factor, most of which rely on a description of the bottom type. The user may select the technique which best applies.

Similarly, the user must program a wind-stress formulation in the subroutine WIND. Values for wind speed and direction are obtained from time-coded data sets using the subroutine INWIND.

Subroutines OPEN, STEADY, OVFL0, and OVFLD supply time-varying values for sea-surface elevation, currents, and overflow conditions at both open and closed boundary points in the grid. In OPEN, an algorithm must be provided to compute the variation of sea-surface elevation along the open boundaries of the grid. The necessary tidal amplitudes are obtained from time-coded sets of data for established tide stations, using subroutine INTIDE. STEADY permits currents to be assigned to individual grid points,

overriding the computed currents. An initial current field may be entered using subroutine INCJRR. Finally, OVFLD and OVPLD permit conditions of flooding to be ascertained and modeled at grid points assigned the control value 2.

When implementing the model on various computers and for various purposes, modifications may be necessary in the input/output subroutines START, DIMENS, HEADS, PRINT, PLOT, and SERIES. RESULT may also be modified to compute additional quantities of interest, such as horizontal transports.

3. Computer Implementation

For this study, the numerical model was implemented on an IBM 3033 mainframe computer at the Naval Postgraduate School. Only a few minor language changes were required before the system's Fortran H compiler could be used on the program originally supplied by Hart. Subsequent modifications were made and all jobs were run from remote terminals under the School's interactive time-sharing system.

The system made possible the development of several programs that facilitated preparation of data for input to the model and production of graphic output. Especially useful among these were: MAKEGRID, a program that generates input depth and computation-control grids from digital bathymetric data already available for the area, simplifying the otherwise laborious task of creating a grid on chart overlays; programs that generate predicted tidal amplitudes from constituents, or from data supplied in the NOS Tide Tables; and, ELEVCOMP and CURRCOMP, programs that plot time-series output from the model against observed data from the same time period for verification of model accuracy. Although the programs themselves may not be transferable to other computers, supplying similar auxiliary software together with the model (or even incorporating the

algorithms into the model program) greatly enhances the ready application of the model to other coastal areas.

Data necessary to running the numerical model were stored in computer files distinguished by type. All constant, gridded data were stored in one file while time-varying data were stored in separate files by type and year (for example, MONTEREY TIDE76). In this way, a new file of input data did not have to be created for each run of the model. The sources and selection of input data are discussed in sections 3.B and 3.C.

III. APPLICATION OF THE MODEL TO MONTEREY BAY

A. VALIDITY OF ASSUMPTIONS

The applicability of the numerical model to Monterey Bay was checked by examining the assumptions outlined in section 2.A. The assumption of negligible vertical velocity was confirmed for tidal forcing by noting that the maximum depth of the area modeled is much less than the wavelength of the semidiurnal tide ($3 \text{ km} \ll 7600 \text{ km}$). Other, horizontal, forcing conditions of currents and wind were applied as steady-state phenomena in the model. In addition, since this study concerns large-scale fluid motions over time periods of 15 minutes or more, short-period turbulent effects and vertical accelerations were neglected: the hydrostatic approximation holds.

Although Monterey Bay is not vertically well-mixed [Scott, 1973], in depths of a few hundred meters or less the difference in dynamic height between that of the assumed, homogeneous density profile and that of a more typical profile is less than 1 cm, which is negligible for the purpose of this study. In depths of 1000 m or more, the effect is more significant (several centimeters); however, since such depths occur outside the bay proper, the effect of density stratification was ignored and horizontal velocities were averaged over depth to obtain a general picture of circulation in the bay.

B. CONSTANT INPUT

The numerical model was applied to three different grids covering Monterey Bay (Figure 1.1 and Figures 3.1 - 3.3). Grid A, a small-scale, 1- or 2-km grid, 80 by 80 km, was

designed to permit the introduction of offshore, non-tidal currents as a steady forcing condition and to place the bay far enough away from the three open boundaries to remove their associated spurious effects. Since this grid was particularly vulnerable to numerical instabilities in the model, two other grids were devised. Grid B, a large-scale, 1-km grid, 23 by 50 km, covered the bay and reduced the number of open boundaries to one. Grid C, a 1-km grid, 40 by 72 km, covered both the bay and sufficient area to permit offshore, non-tidal currents to be introduced. All grids were skewed 20° east of north to align the boundaries perpendicular to the tidal forcing conditions. The dimensional and constant data incorporated into these grids are discussed below.

1. Time and Space Dimensions

A time step of one hour was chosen to permit assessment of the model over periods of several days without necessitating extensive use of CPU time. Normally the model should run for 12-24 hours (one tidal cycle or more depending on the tidal phase differences between various parts of the area) to establish realistic conditions of current and sea-surface elevation throughout the area [Hart, 1976]. The one-hour interval provided a sufficient number of data values for comparison with hourly or half-hourly observations of sea-surface elevation and currents.

Since computed values are offset in the staggered-grid scheme of the model, use of a relatively small grid size in regions of steep bathymetric relief is important to model accuracy. With the constraint on array dimensions in mind, the smallest grid size possible (1 km²) was generally selected to permit the greatest spatial resolution for the area of concern.

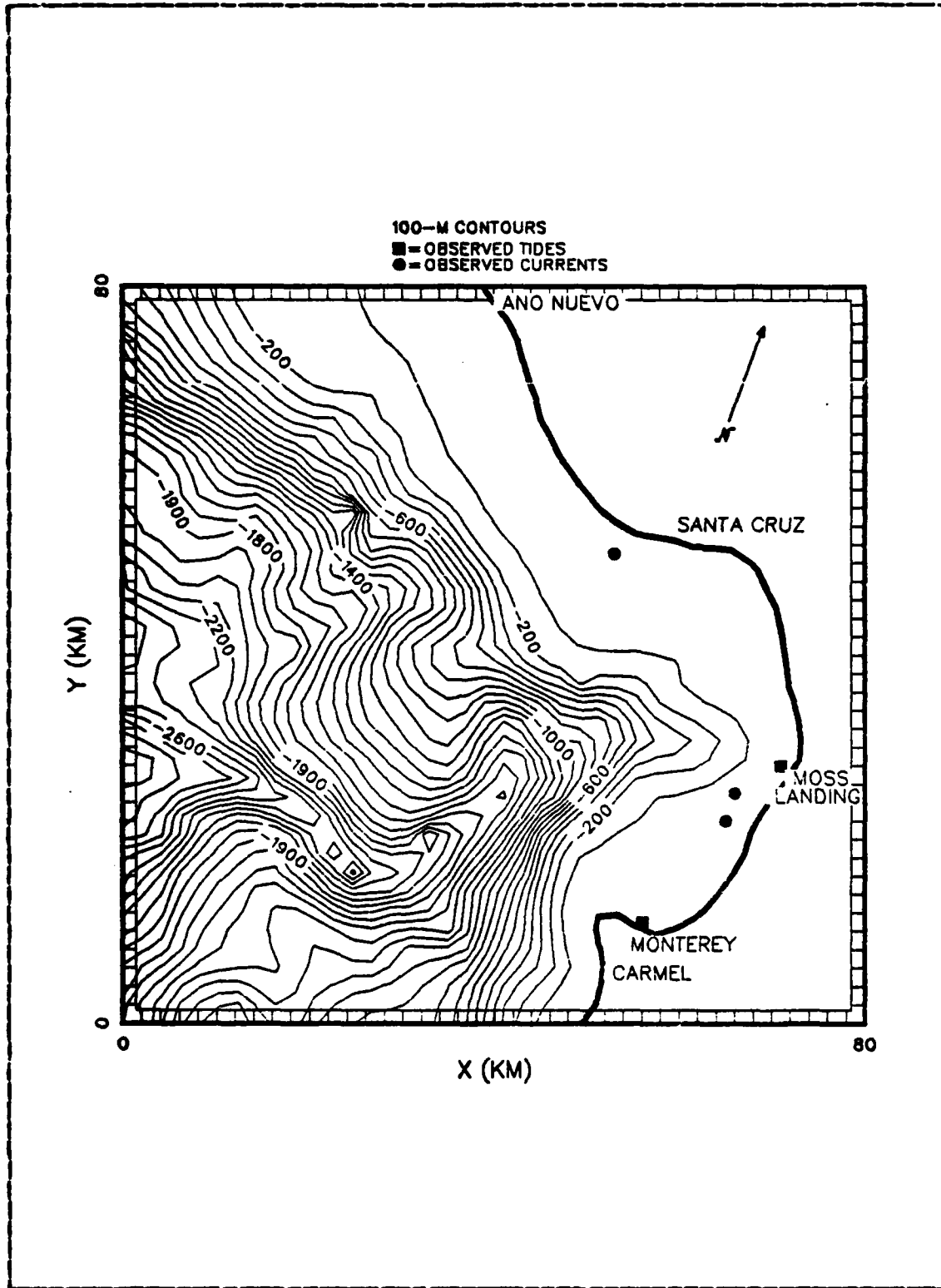


Figure 3.1 Depth Contours for Grid A.

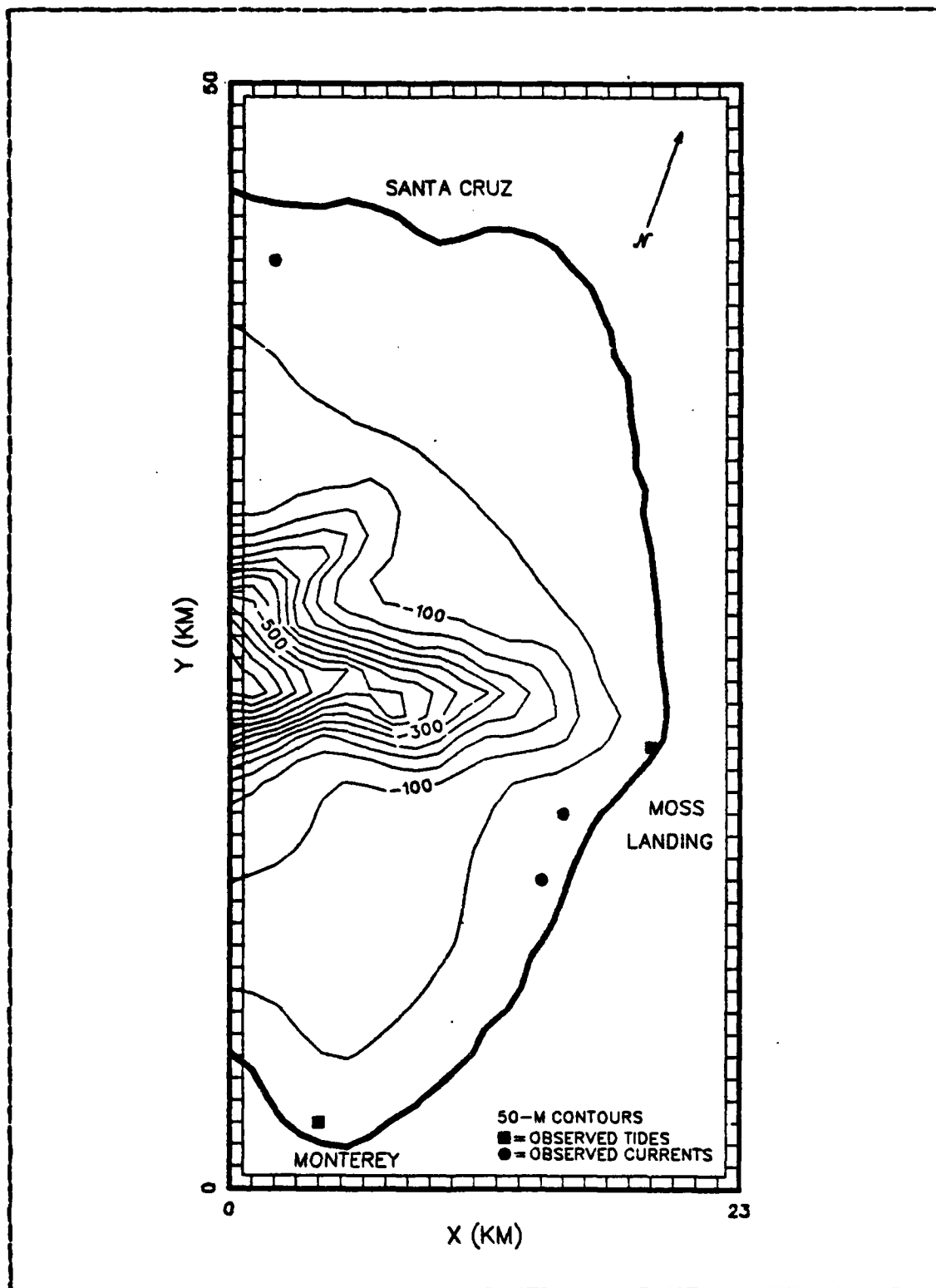


Figure 3.2 Depth Contours for Grid B.

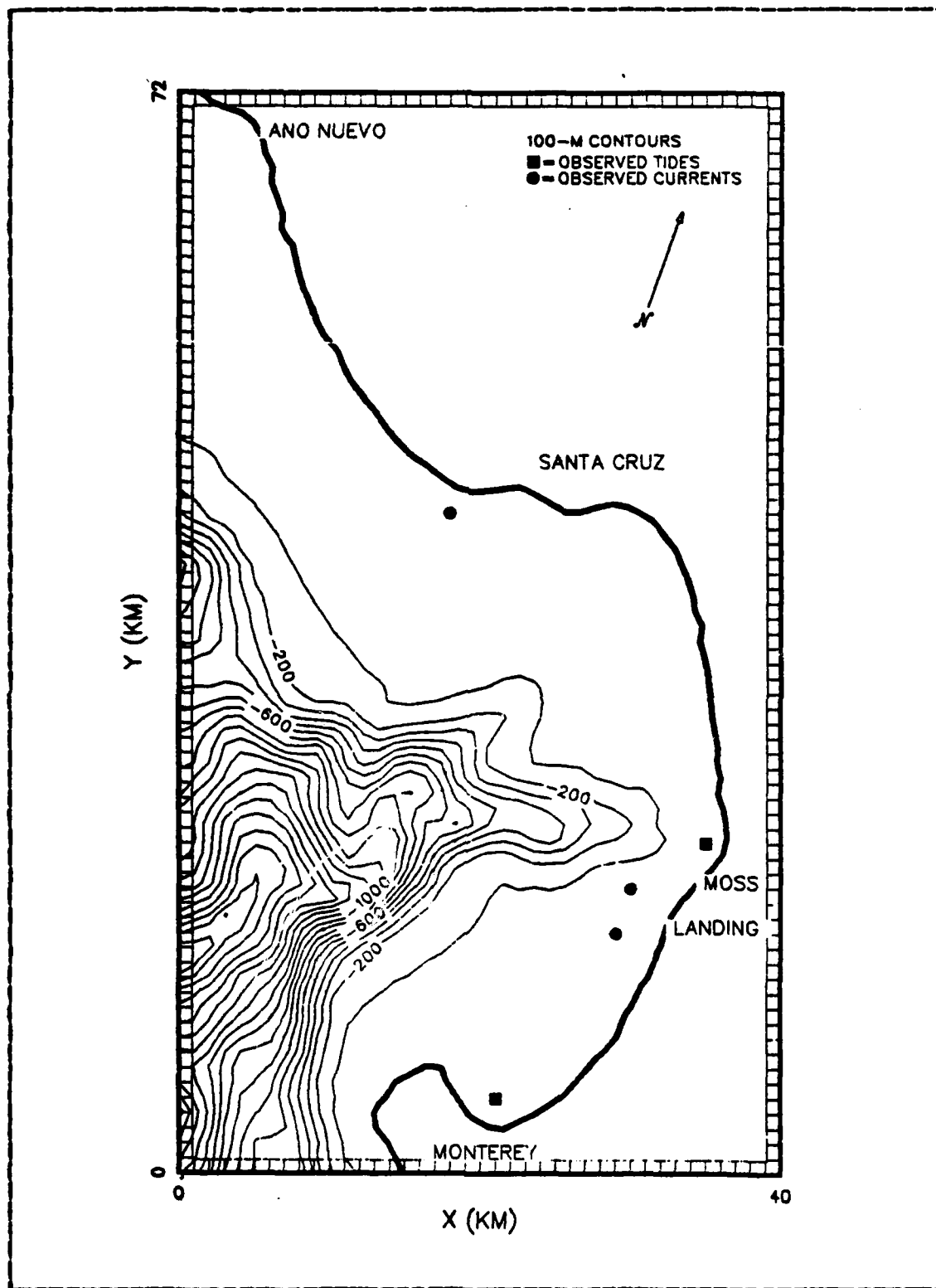


Figure 3.3 Depth Contours for Grid C.

2. Bathymetry and Datum

Digital bathymetry was provided by the NOAA National Geophysical Data Center, where depth data from past hydrographic surveys are archived for most coastal areas of the United States. The depths were positioned by latitude and longitude in a 36-sec grid and were referenced to a mean-lower-low-water (MLLW) datum.

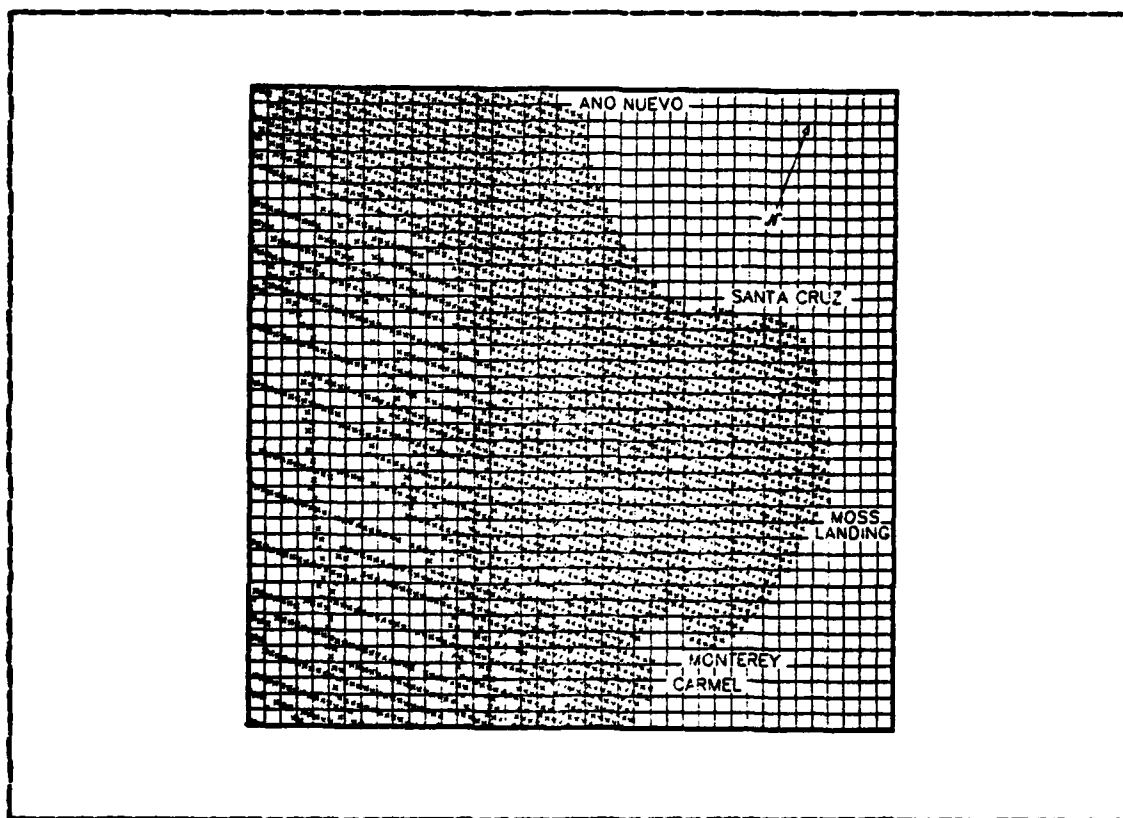


Figure 3.4 Locations of Bathymetric Data in Grid A.

To computer-generate a grid of depths for the model, the program MAKEGRID was prepared. The program first projects the bathymetric data onto the grid coordinate system (for example, grid A), which is a modified-transverse Mercator projection skewed about a specified origin

(Figure 3.4). Depths are then interpolated at the corners of each grid square.

Since depths are referenced to MLLW and a straightforward correction to mean sea level is not possible, the datum for sea-surface elevations computed by the model was taken to be MLLW. All input tidal amplitudes were likewise referenced to MLLW.

From the gridded depths a computation-control grid was automatically generated by assigning 1's to all water squares and 0's to all land squares (assigned dummy elevations in the depth grid). Both grids could be altered if necessary before their use in the model.

3. Bottom Friction

To model bottom stress, the empirical Manning equation for the Chezy coefficient, C, was used:

$$C = (h+\eta)^{1/6}/M \quad (3.1)$$

The coefficient is a function of depth, h, instantaneous sea-surface elevation, η , and the Manning factor, M, which describes bottom roughness. M increases with bottom roughness. Clean and straight natural river channels typically require $M=0.025$ to 0.030 m/s, while winding channels may require $M=0.033$ to as high a value as 0.15 m/s in very weedy, overgrown areas [p. 99, Henderson, 1966].

Although bottom stresses may be modeled as a function of the bottom type or texture in each grid square (thus requiring input of a bottom-type grid), this option was not exercised for Monterey Bay. Over the large area covered, the variation in depth from square to square is likely to have more influence than the relatively small variations in bottom roughness that occur in Monterey Bay. Following Spaulding and Beauchamp's study of a coastal sea (1983) and

after some experimentation (section IV.A), a constant value of $M=0.04$ m/s was used throughout the bay.

C. TIME-VARYING INPUT

The forcing conditions of tide and wind were accessed from time-coded files. Tidal amplitudes were applied only along the open boundaries of the model, whereas wind stress was applied over the entire grid. The sources and application of these data are discussed in this section.

1. Initial Conditions

At the start of a run of the model, sea-surface elevations were approximated by assigning a coastal tidal amplitude at the starting time to every point in the grid. The tidal amplitude at Monterey was used for this purpose. This approximation is suitable for Monterey Bay since the narrow continental shelf and the absence of any barrier islands permit the tidal wave to propagate relatively rapidly through the area.

A zero velocity was initially assigned to each grid point, except for runs including an offshore, non-tidal current; in these cases, the steady-state current velocity was initially assigned to offshore grid points.

2. Boundary Tidal Amplitudes

A major factor in the successful application of the numerical model was the provision of suitable tidal forcing conditions along the open boundaries. Tidal amplitudes are predicted in the NOS Tide Tables 1976 for four stations near and within Monterey Bay: Ano Nuevo, Santa Cruz, Monterey, and Carmel. Tidal-constituent amplitudes and phases are available for Monterey and Moss Landing (Appendix A). Since 1963, continuous observations of water level have been made

at Monterey. A two-year series of nearly continuous observations was made at Moss Landing from 1976 through 1977. To obtain amplitudes along the boundaries of the model grid, coastal values such as these must be extrapolated.

Several attempts have been made to formulate the effects of continental shelves on the open-ocean tide [Clarke and Battisti, 1980; Gill and Porter, 1980; Munk, et al., 1970]. Because of the narrow continental shelf and bisecting canyon, Monterey Bay does not satisfy the assumptions necessary to apply these formulations. However, to gain some insight into the effect of the extreme depth difference between the tide station at Monterey and the offshore boundary points of the model, a comparison was made between tidal constituents obtained at Monterey and at a pressure gage located in 3903 m of water offshore [Cartwright, et al., 1979]. The results are presented in Table II.

The coastal and pelagic phases clearly do not correspond since the pelagic gage was located at some distance from Monterey (see Figure 1.1), but the agreement of the amplitudes suggests that the aforementioned depth difference has little effect. In the absence of any more certain method for extrapolating tidal amplitudes, the values at the coastal station were applied directly along a line of constant phase extending out from shore.

Examination of cotidal/cophase charts by Munk, et al. (1970), Luther and Wunsch (1975), and Parke and Henderschott (1980), suggests that, in the vicinity of Monterey Bay, the tidal wave propagates nearly parallel to the coast. The model grids were, therefore, skewed in such a way that the open boundaries were perpendicular or parallel to the coast. At each time step the forcing amplitude was made to vary directly with the tide at Monterey all along the southern boundary, with the tide at Ano Nuevo all

TABLE II
Comparison of Pelagic and Coastal Tidal Constituents

	Monterey 36°36'N 121°53'W 8 m	Pelagic 38°09'N 124°54'W 3903 m
H (cm)		
M ₂	50	55
S ₂	13	13
N ₂	11	13
K ₂	4	--
K ₁	37	43
O ₁	23	28
P ₁	12	--
Q ₁	4	--
k (°)		
M ₂	297	66
S ₂	296	84
N ₂	272	30
K ₂	288	--
K ₁	98	334
O ₁	81	321
P ₁	93	--
Q ₁	73	--

along the northern boundary, and with linearly interpolated values between the two along the western boundary.

The tidal values used to set the boundary conditions may be interpolated from the NOS Tide Tables 1976, computed from constituents [Schureman, 1940], or taken directly from observed data. The last was preferred since the first two predictive techniques cannot take into account atmospherically forced or anomalous changes in sea level, such as storm surge. However, as mentioned previously, observations were available only at Monterey and Moss Landing. Some experimentation was necessary to model the phase lags between Monterey, Santa Cruz, and Ano Nuevo (section IV.A).

3. Boundary Currents

Two types of flow may be imposed at the boundaries of the numerical model. First, the discharge of rivers along otherwise closed boundaries may be represented as a vertically averaged current velocity assigned to the appropriate coastal grid point during each time step. The mean annual discharge of all major streams and rivers entering Monterey Bay is $1.85 \times 10^6 \text{ m}^3/\text{day}$ [Broenkow and Smethie, 1978], which amounts to a vertically averaged current velocity of only 0.2 cm/s were all rivers to enter at one point. As a result, the river inflow was judged negligible for this application.

A second type of flow, currents due to non-tidal effects, may be imposed in offshore regions of the model. The narrowness of the continental shelf near Monterey Bay leaves the bay particularly open to forcing by large-scale oceanic currents. Previous studies of the area suggest that such currents are an important force driving the circulation of the bay [Lazanoff, 1971; Garcia, 1971; Bretschneider, 1982]. The presence of an offshore current was simulated by assigning initial velocities to the offshore portion of grids A and C for some runs of the model. The convective-inertia terms in the numerical model propagate the current influence into the inshore portions of the grid. A northward current of 25 cm/s (0.5 knots) was assigned. This value was proposed by Scott (1973) as a simple, steady-state model for the offshore circulation.

4. Wind

Wind stress, F_i , was parameterized within the numerical model by the familiar quadratic law [Dronkers, 1964]:

$$F_i = (2.6 \times 10^{-3}) \rho_a W |W| / \rho (h + \eta) \quad (3.2)$$

W represents the wind velocity vector, ρ_a is atmospheric pressure, ρ is the mean density of the water, h is the depth, and η is the time-varying sea-surface elevation. The model permits input of wind direction and amplitude as a forcing condition over the whole field of the grid for a specified range of time steps. Monthly distributions of wind at Santa Cruz and Moss Landing for the period May, 1976, through May, 1977, were obtained from the Santa Cruz Wastewater Facilities Planning Study [Brown and Caldwell, Inc., 1978]. Average and maximum values for the wind were applied to some runs of the model (see section IV.B).

D. DATA FOR COMPARISON

The numerical model was calibrated by comparing modeled sea-surface elevations and current velocities at specific grid points with observed values at the same locations. The comparison process was limited by a paucity of suitable, long-term water-level and current-meter observations for Monterey Bay. Water-level data are available only for National Ocean Service tide stations at Monterey and Moss Landing. The primary sources for current-meter data are predesign studies conducted for the emplacement of sewage outfalls near Santa Cruz, the Pajaro River, and the Salinas River, but only data for Santa Cruz and the Salinas River could be obtained. In some fortuitous instances, both water-level and current-meter data were collected concurrently (Figure 3.5). The period July-August 1976 yielded sufficient data for comparisons at the two water-level and at three current-meter stations; their locations are plotted on each model grid (Figures 3.1 - 3.3).

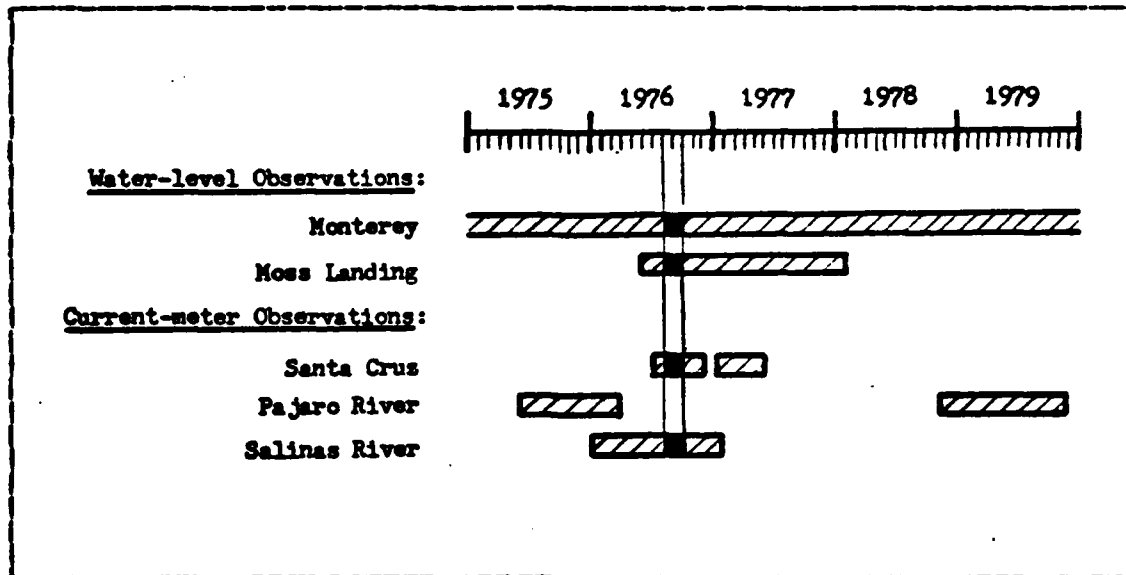


Figure 3.5 Observing Periods for Comparison Data.

1. Water-level Observations

Water-level observations have been made nearly continuously since 1963 at NOS Tide Station 941-3450 on the seaward end of Municipal Wharf 2 in Monterey. The float-type tide gage is located in 8.2 m of water. Recorded times are accurate to within 6 minutes and heights are resolved to 3.0 cm [Bretschneider, 1980]. Digitized hourly heights for the period 11/8/73 to 3/2/83 were obtained from the National Ocean Service, Tidal Datums Section N/OMS123. The heights were corrected to MLLW and converted from feet to meters. In addition to providing comparison data, these observations were used to determine boundary amplitudes for some runs of the model.

At Moss Landing water-level observations were made for 20 months as part of the California Marine Boundary Program [National Ocean Survey, 1981]. NOS Tide Station 941-3616 was a float-type tide gage located at the seaward end of the Moss Landing Ocean Pier in 9.1 m of water.

Digitized hourly heights were obtained for the entire period 5/9/76 to 1/10/78 and processed as for the station at Monterey.

2. Current-meter Observations

As part of the Santa Cruz Wastewaters Facilities Planning Study, a current-meter station was located 1 mile offshore of Terrace Point in 30 m of water [Brown and Caldwell, Inc., 1978]. Two AMF Vector Averaging meters were installed at 9- and 15-m depths for the periods June to November, 1976, and January to May, 1977. The only data that could be obtained for comparison purposes covered July and August, 1976, at the 15-m depth. The data included 7.5-minute averages of current speed and direction, expressed as a pair of orthogonal velocity vectors.

Two current-meter stations were occupied approximately 1 nautical mile north and south of the Salinas River during oceanographic investigations for the Monterey Peninsula Water Pollution Control Agency [Engineering-Science, Inc., 1977]. At each station, two ducted-impeller-type meters were installed at 9 and 15 m for the overall period January, 1976, to January, 1977. Current speeds and direction were averaged at 30-minute intervals and expressed as a pair of orthogonal velocity vectors.

IV. RESULTS

A. COMPARISON OF MODEL RESULTS WITH OBSERVATIONS

Comparison of the model with observations was used both to "fine tune," or calibrate, the numerical model, and to assess its general validity. The effects of varying input constants such as the size and resolution of the grid, the time step, and the bottom-friction coefficients were considered. In addition, schemes for determining boundary tidal amplitudes and for including non-tidal current fields were tested in an effort to match observed elevations and currents as closely as possible.

Application of the model to grid A revealed apparent numerical instabilities that caused overflow in the computations after as few as 1.25 days (30 time steps). The sudden oscillations in sea-surface elevation at Monterey were due to propagation into the bay of extreme amplitudes and currents generated in the offshore portion of the grid (Figure 4.1). The overflow condition was unaffected by changing the resolution of the grid from 2 to 1 km, but was very sensitive to changes in the phasing of the tidal amplitudes along the open boundaries. Under the premise that the presence of three open boundaries enhanced instabilities, grid B (with one open boundary) and grid C (with two open boundaries) were subsequently used during the comparison process.

1. Sea-surface Elevation Comparisons

A run of the model for twelve days at the one-hour time step produced some agreement between modeled and observed sea-surface elevations at Monterey and very good

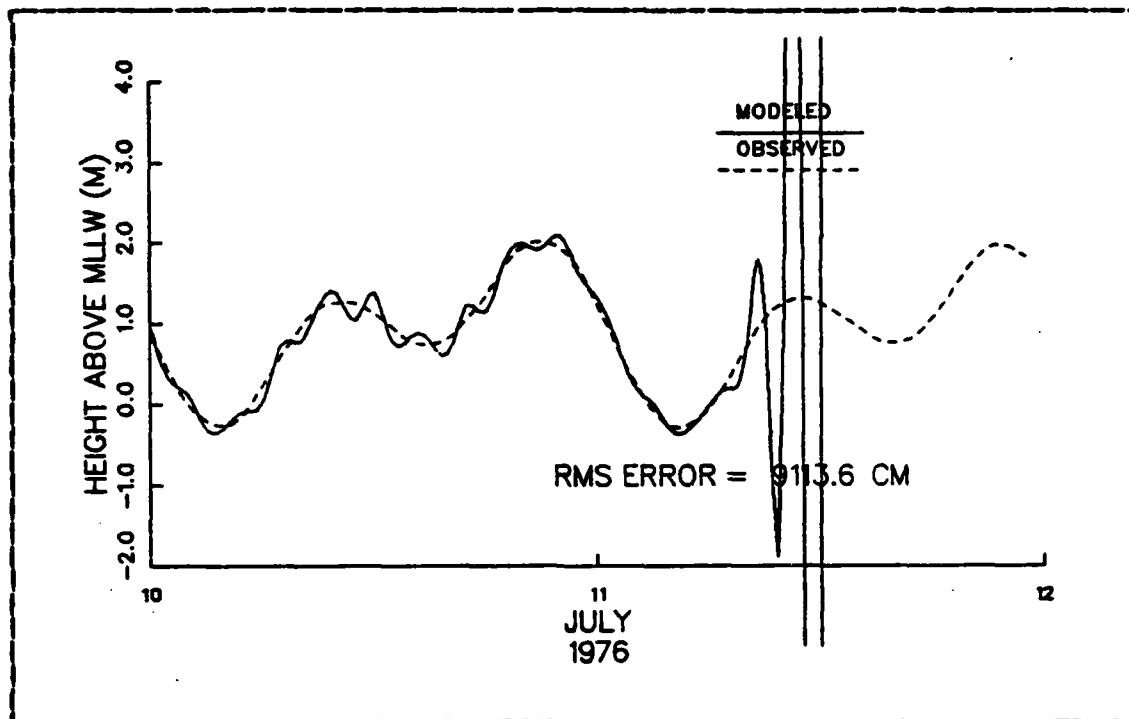


Figure 4.1 Sea-surface Elevations at Monterey, Grid A.

agreement at Moss Landing (Figures 4.2 and 4.3). Varying the Manning bottom-friction factor improved this result (Table 3.1 and Figures 4.4 and 4.5).

TABLE III
Effect of Various Manning Factors

M (m/s) =	.03	.04	.05	.06	.10
Monterey	7.4	6.8	6.3	5.8	4.8
Moss Landing	4.6	4.5	4.4	4.3	4.0

Table values are the RMS errors in centimeters for comparisons between modeled and observed sea-surface elevations.

The seemingly unrealistic Manning factor of 0.10 m/s may serve as a description of the bottom roughness over the large area of each grid square, if roughness is thought of in terms of the steep slope that is otherwise not accounted for in the model. The higher Manning factors did not, however, improve the results of current comparisons; they served primarily to damp out noise.

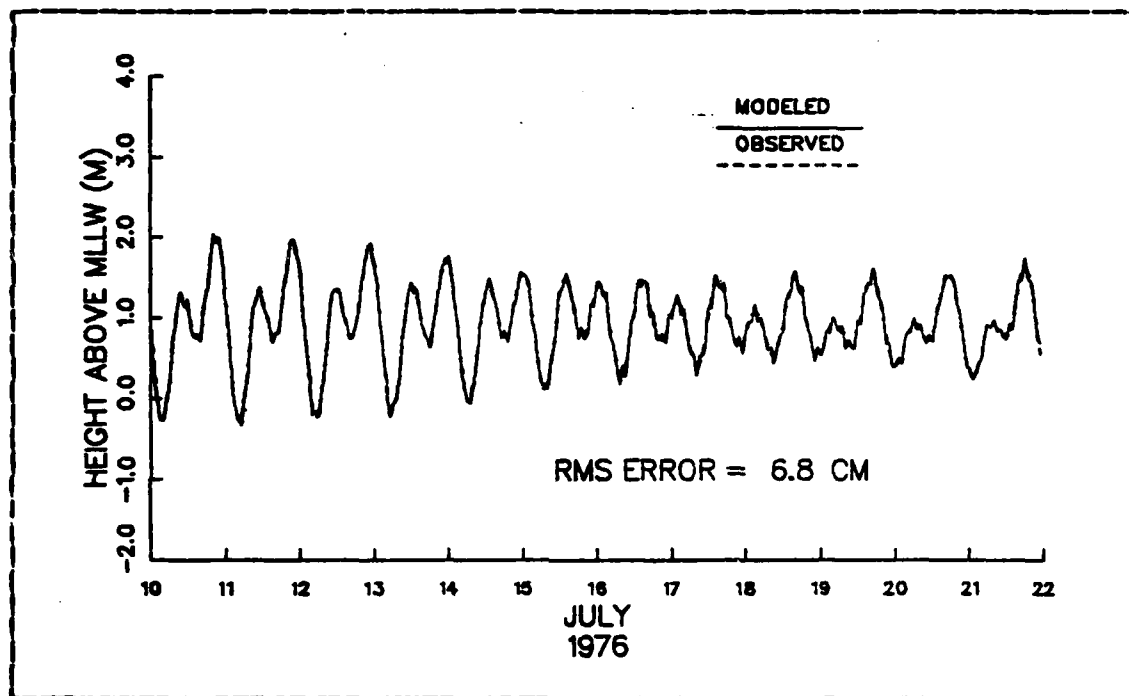


Figure 4.2 Elevations at Monterey, $\Delta t=3600$ s.

An oscillation that appeared forced by the time step was evident in the modeled curves. It was especially evident at Monterey and when a shorter, 15-minute time step was used (Figures 4.6 and 4.7).

The noise may be the result of applying observed tidal amplitudes as the boundary forcing condition. The observed water levels, digitized hourly, may include jumps and/or contaminating frequencies due to the recording

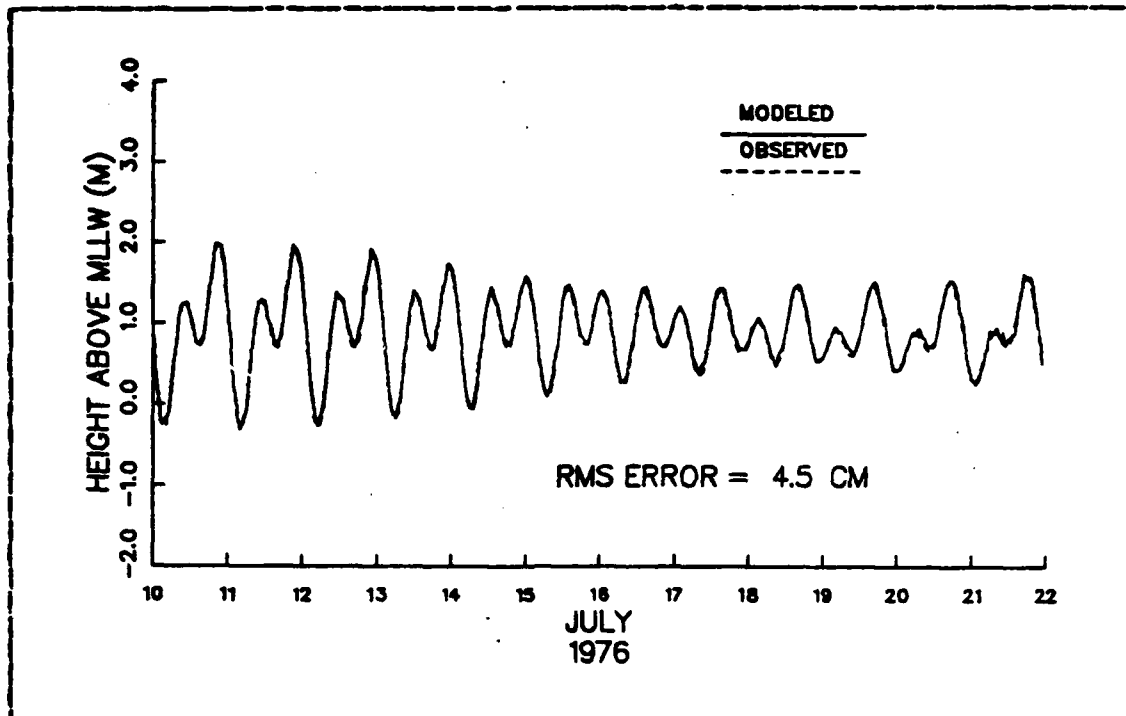


Figure 4.3 Elevations at Moss Landing, $\Delta t=3600$ s.

instruments. Linear interpolations required between the hourly amplitudes for each half time step may have exaggerated the instrumental effects. To better judge the use of a shorter time step, raw water-level observations, usually made at a 6-minute interval, should be applied to the model.

Spectral analysis of the modeled and observed curves, in addition to reflecting their general agreement, reveals spurious frequencies generated by the model at Monterey (Figures 4.8 and 4.9). The incoherent frequencies, which are also found in the spectra for currents at Santa Cruz (Figure 4.14), correspond to apparent periods of 3.0 and 2.2 hours. These periods are longer than the 1-hour, fundamental seiche period for Monterey Bay [Lynch, 1970].

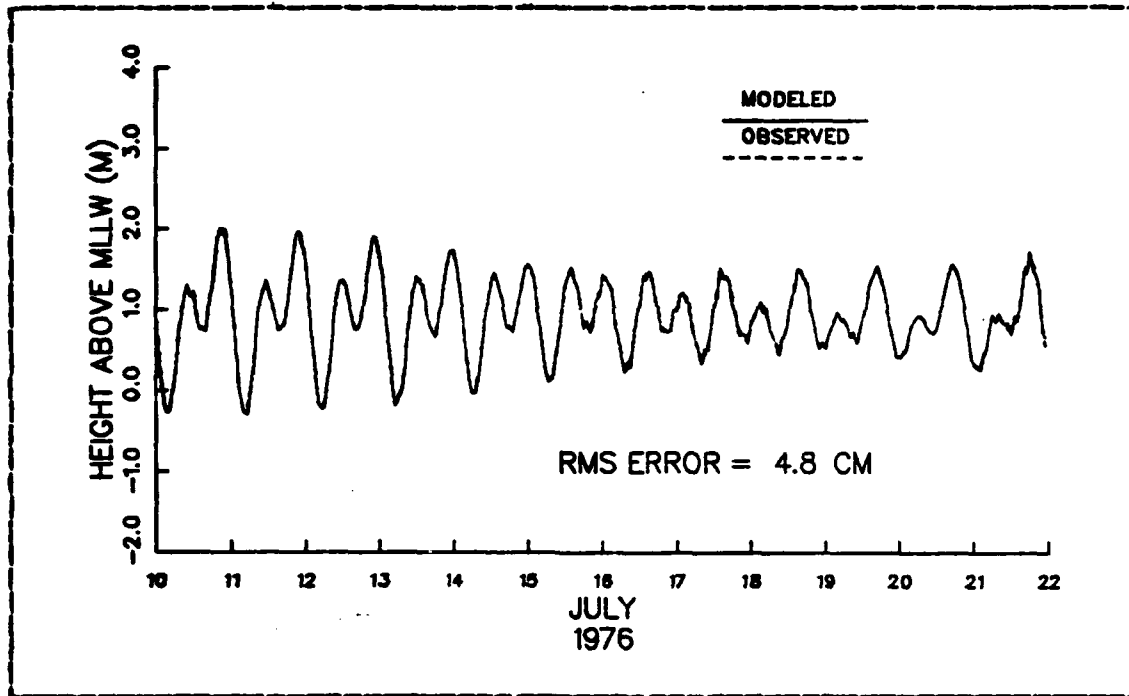


Figure 4.4 Elevations at Monterey, $M = .10$ m/s.

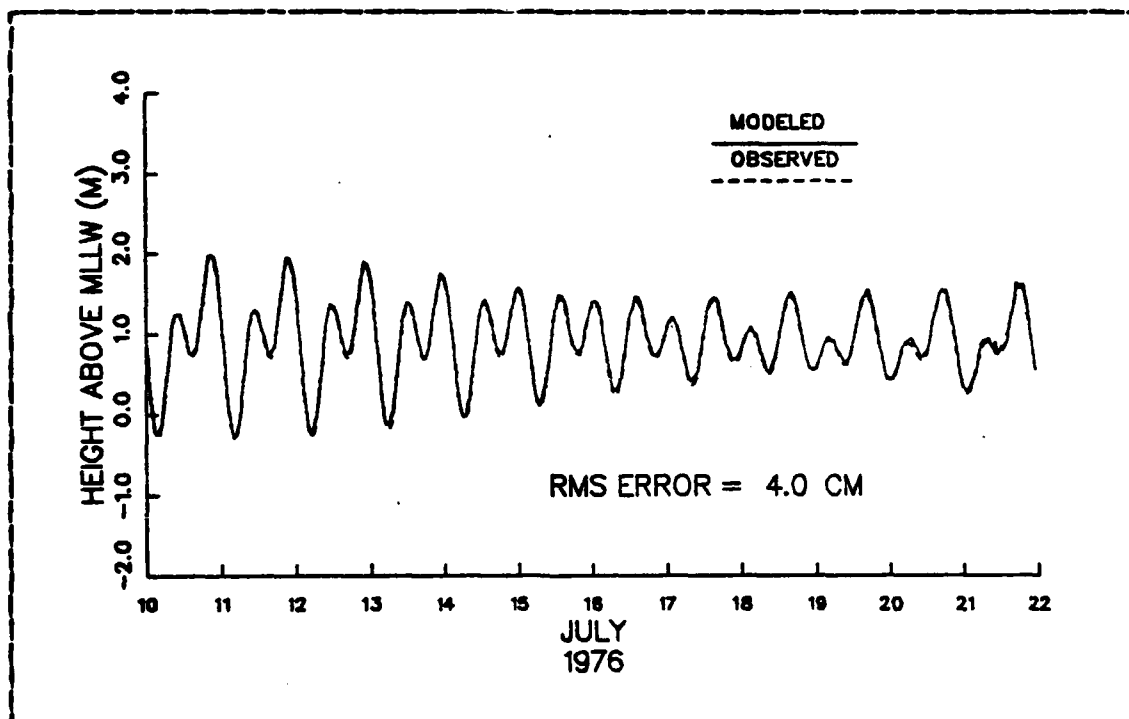


Figure 4.5 Elevations at Moss Landing, $M = .10$ m/s.

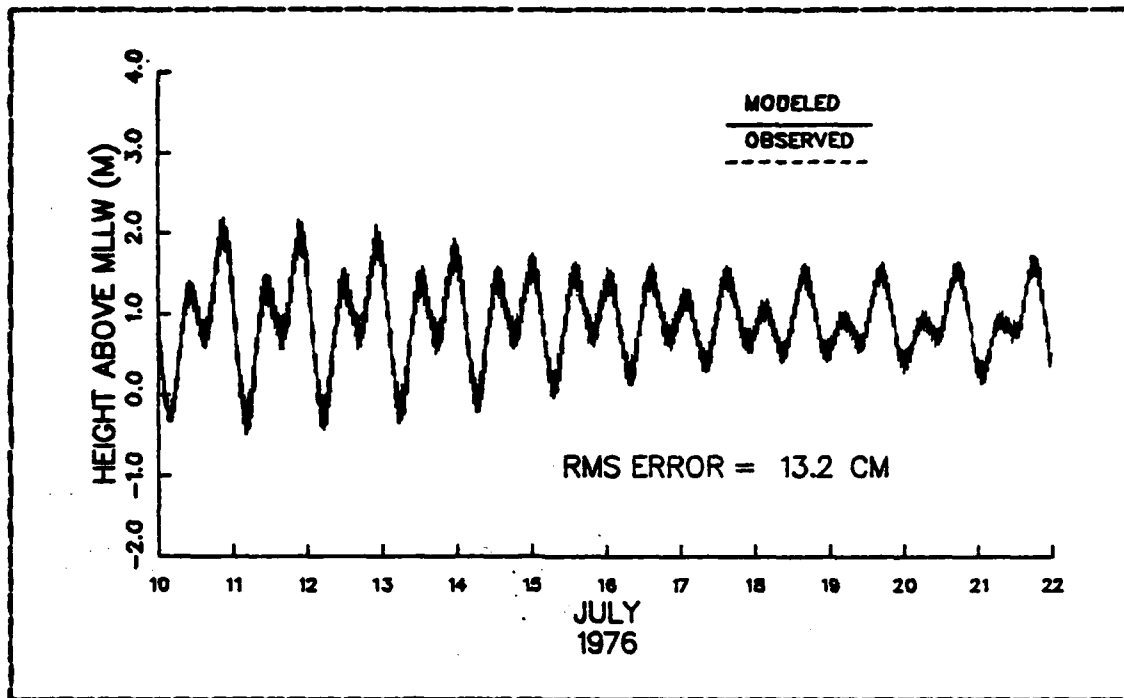


Figure 4.6 Elevations at Monterey, $\Delta t=900$ s.

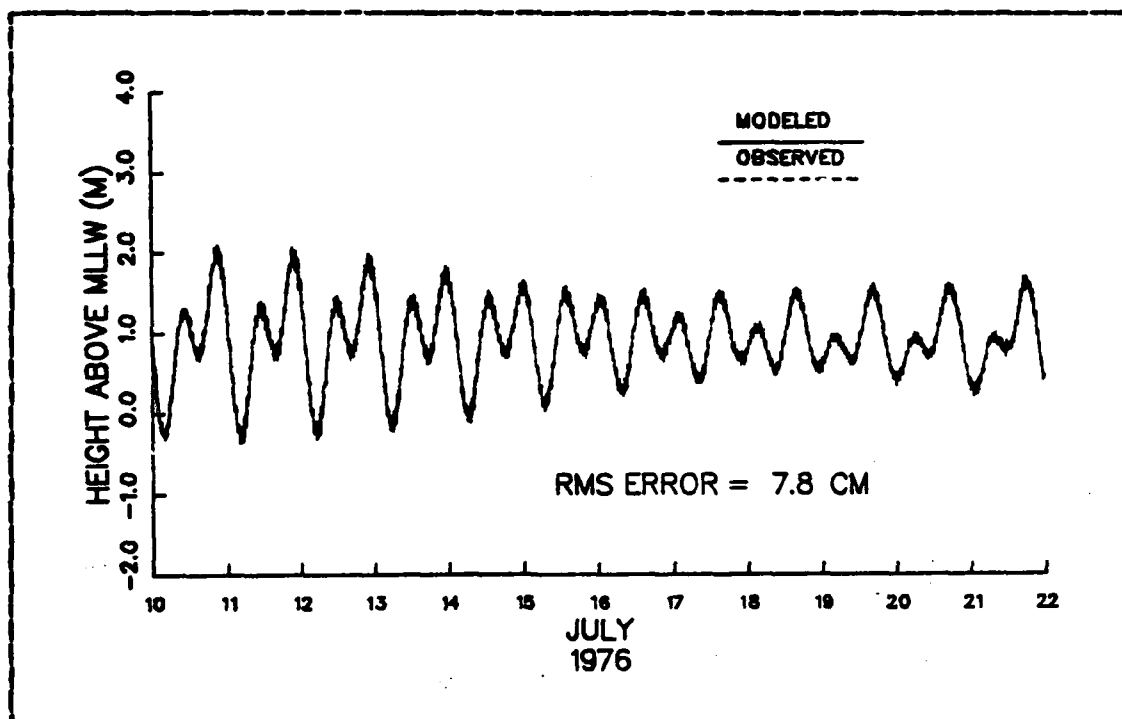


Figure 4.7 Elevations at Moss Landing, $\Delta t=900$ s.

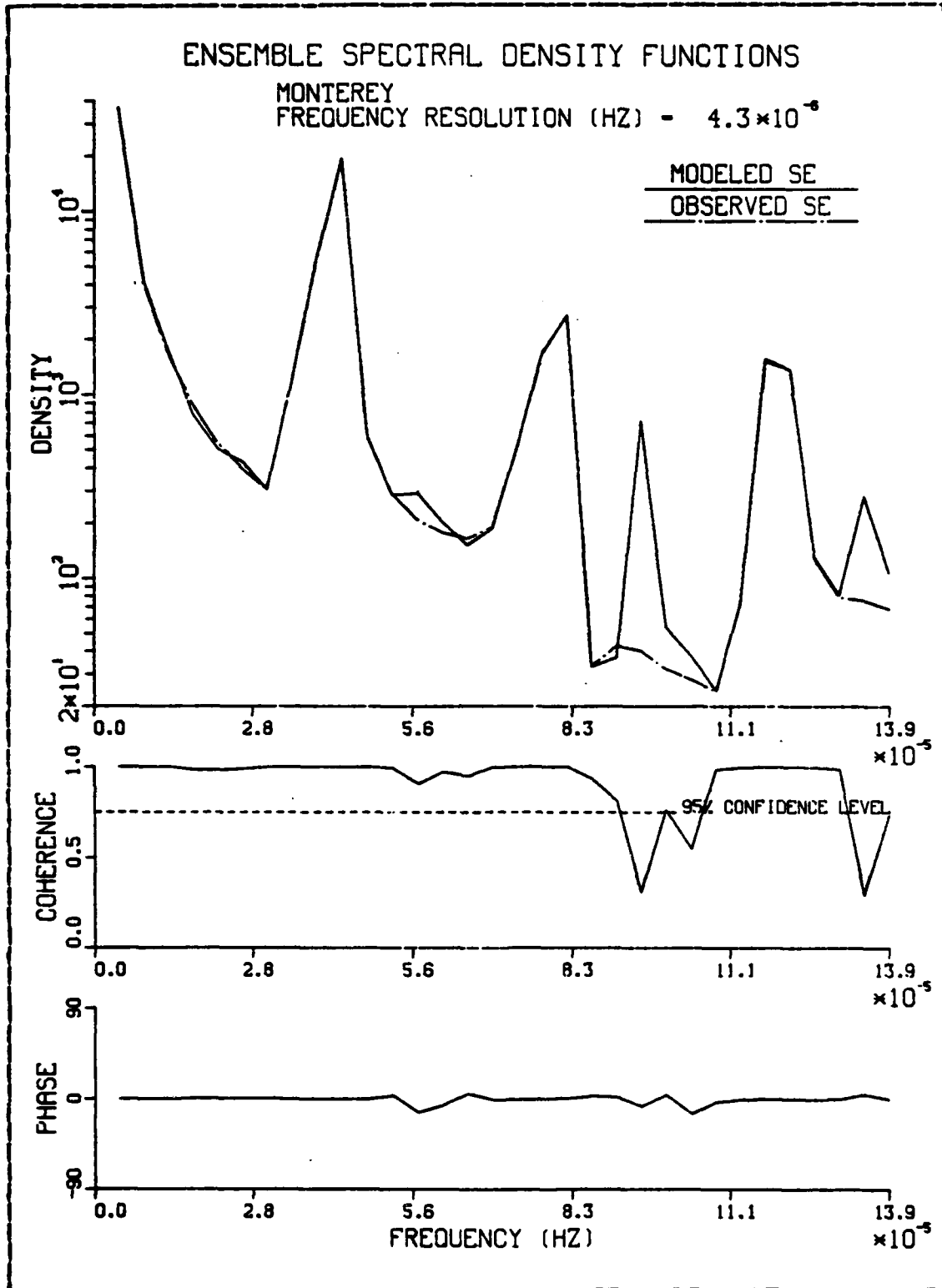


Figure 4.8 Spectra, Elevations (SE) at Monterey.

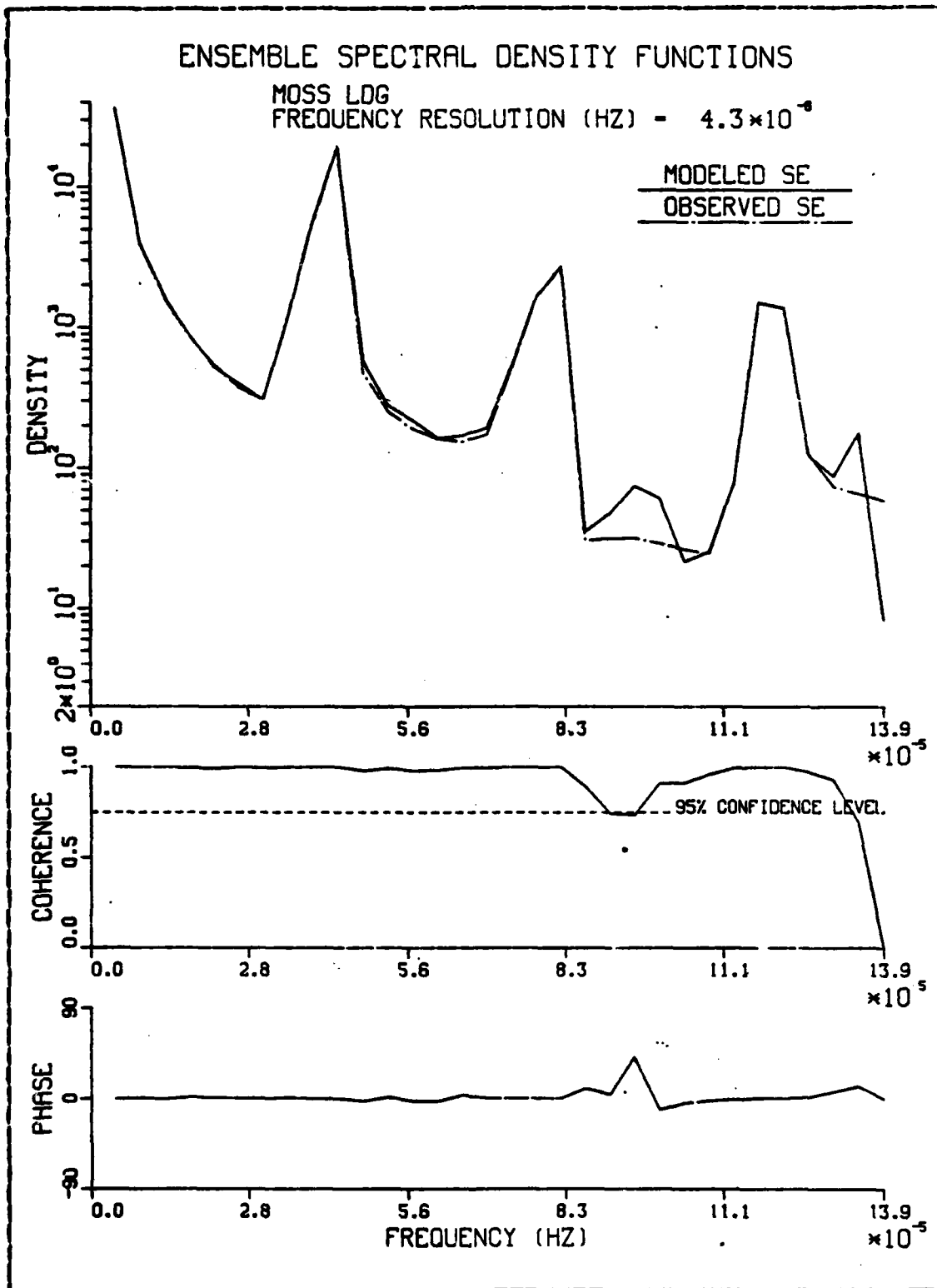


Figure 4.9 Spectra, Elevations (SE) at Moss Landing.

The phenomenon of time-step-linked oscillations has been experienced by other investigators [Chiang and Lee, 1982], who found that generating a mathematically smooth function from the observed data provided more suitable amplitudes for forcing the model. A smooth amplitude function was obtained in this study by summing the tidal constituents for Monterey. Applying boundary conditions based on these predicted tides gradually reduced the noise in the model (Figure 4.10). Not surprisingly, however, the predicted elevations did not provide good agreement with the observed water-levels.

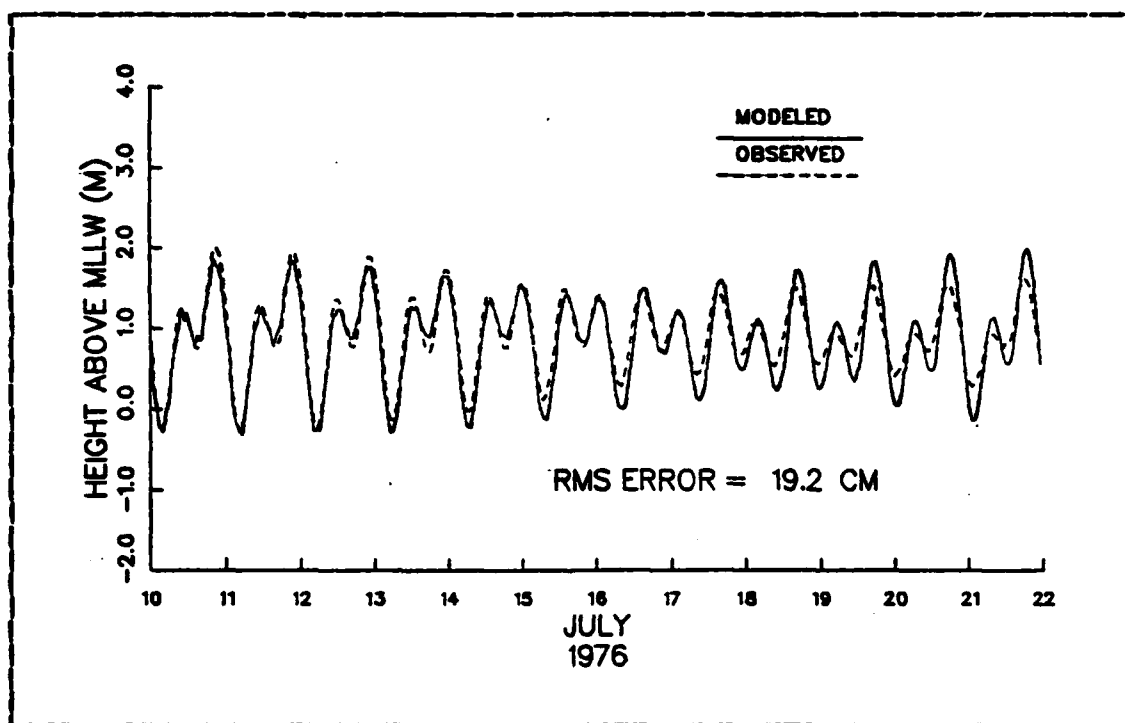


Figure 4.10 Elevations Using Predicted Boundary Amplitudes.

The sensitivity of the model to open-boundary conditions, already noted in the case of grid A, was demonstrated by comparing results for different phase lags along the one

boundary of grid B (table IV). A constant amplitude along the boundary (no phase lag) was found to be most successful, though the NOS Tide Tables 1976 predict that Monterey lags Santa Cruz by 6 minutes.

TABLE IV
Effect of Boundary Amplitude Phasing on Grid B

Phasing	6+	0	6-
Monterey	7.9	7.4	7.8
Moss Landing	5.3	4.6	5.0

Table values are the RMS errors in centimeters. Phasing is Monterey minus Santa Cruz, in minutes.

2. Current Comparisons

The model-generated current values agreed poorly with the 15-m depth observations at all three locations where comparisons were made (Figures 4.11-4.13). In making the comparisons, current vectors from the model output and from the observed records were resolved into eastward and northward components, taking into account their respective skewed coordinate systems. The modeled current components, particularly near the Salinas River mouth, were weak or non-existent. Clearly, forces in addition to tides were at work in generating the observed currents.

For the currents near Santa Cruz the apparent rough correspondence in frequency was confirmed somewhat by a spectral analysis (Figure 4.14). The gradual increase in the northward component of the modeled current may reflect long-period variations in the current field.

In an effort to obtain better current agreement and to see the effects of currents associated with the continental slope, a steady offshore current was applied to grid C. The results near Santa Cruz were poor; inherent oscillations in the model were amplified and agreement was not improved. The model's sensitivity to open-boundary conditions made this a difficult subject to pursue within the scope of this study.

B. MODELED CIRCULATION OF MONTEREY BAY

Although the tidally forced numerical model did not reproduce observed currents at the comparison locations, it should nevertheless provide an estimate of the barotropic tidal circulation of Monterey Bay. A general view of circulatory patterns may be obtained by examining the modeled sea-surface elevation and current fields for a 24-hour period.

1. Tidally Forced Circulation

A tidally forced elevation-field series is presented in Appendix B. A small oscillatory structure in the southern bight is consistent with the greater amplitude of noise observed at Monterey. In other respects, the elevation fields generally show a clear progression of the tidal wave into the bay.

A series of current-field plots, including the volumetric transport associated with each vector, is presented in Appendix C. A total volume of $2.0 \times 10^9 \text{ m}^3$ appears to be pumped across the boundary during the diurnal tidal cycle. This barotropic result may be contrasted with the 10^9 m^3 pumped by internal tidal mixing reported by Broenkow and Smethie (1978).

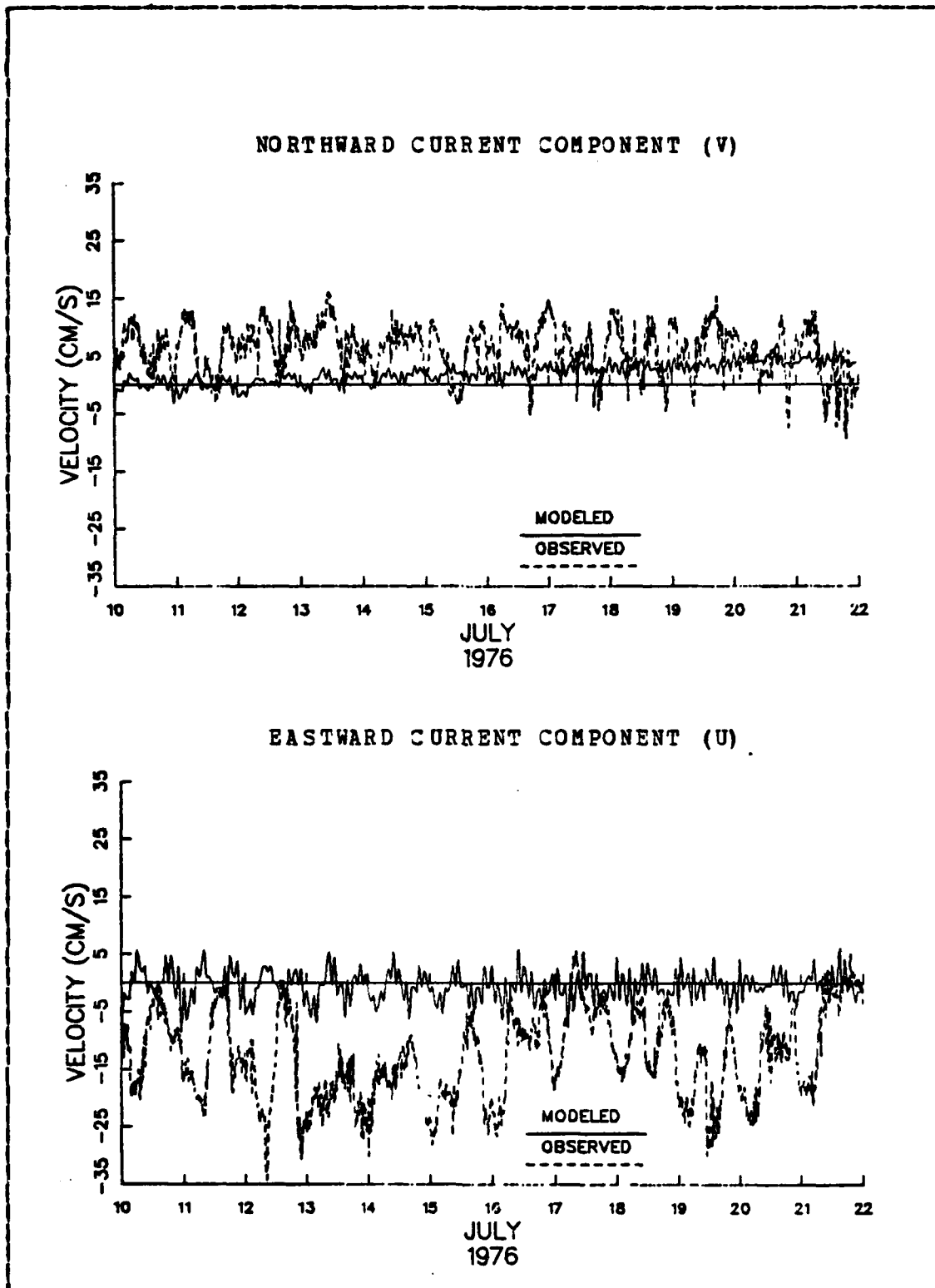


Figure 4.11 Currents near Santa Cruz.

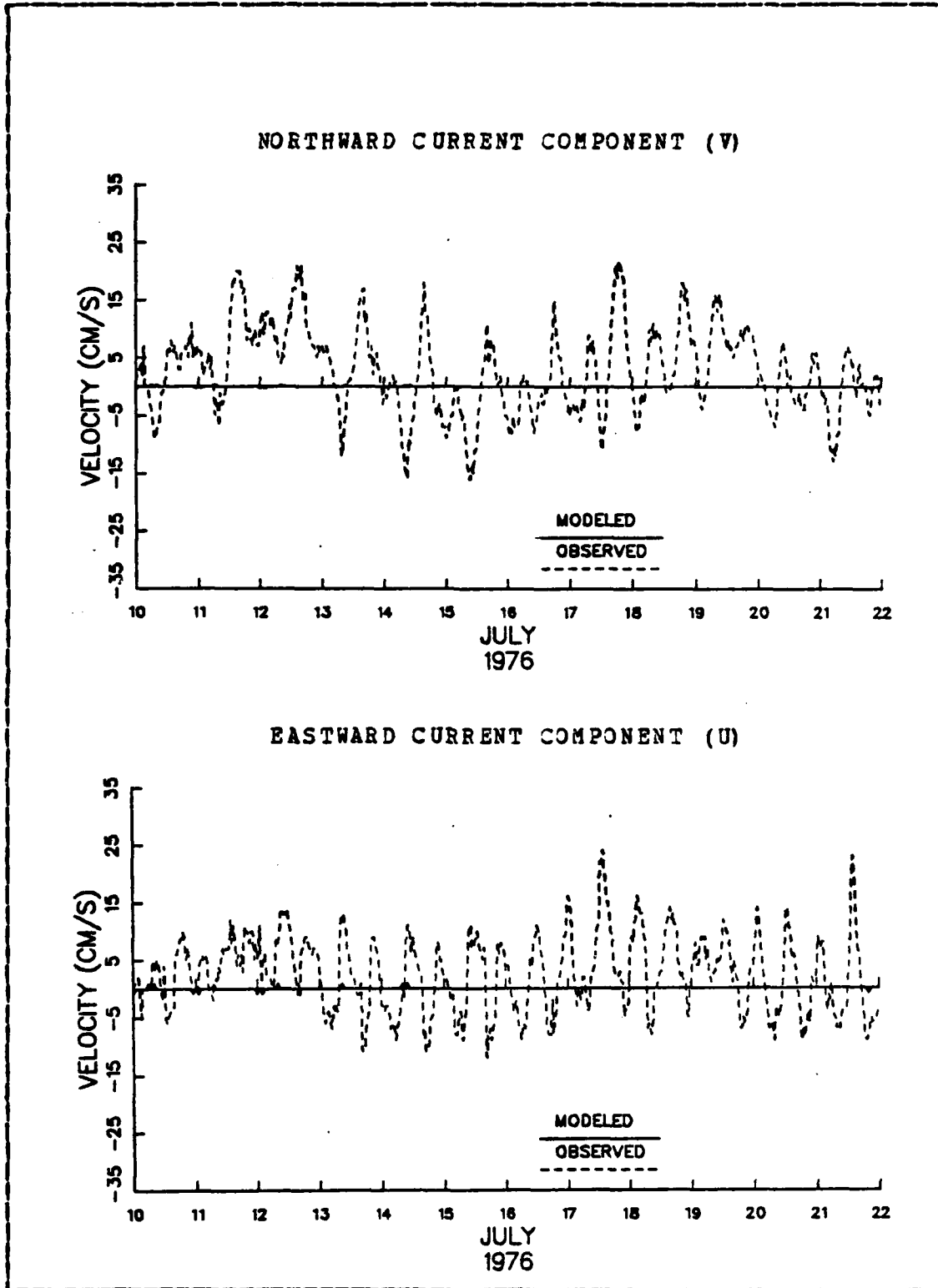


Figure 4.12 Currents South of the Salinas River.

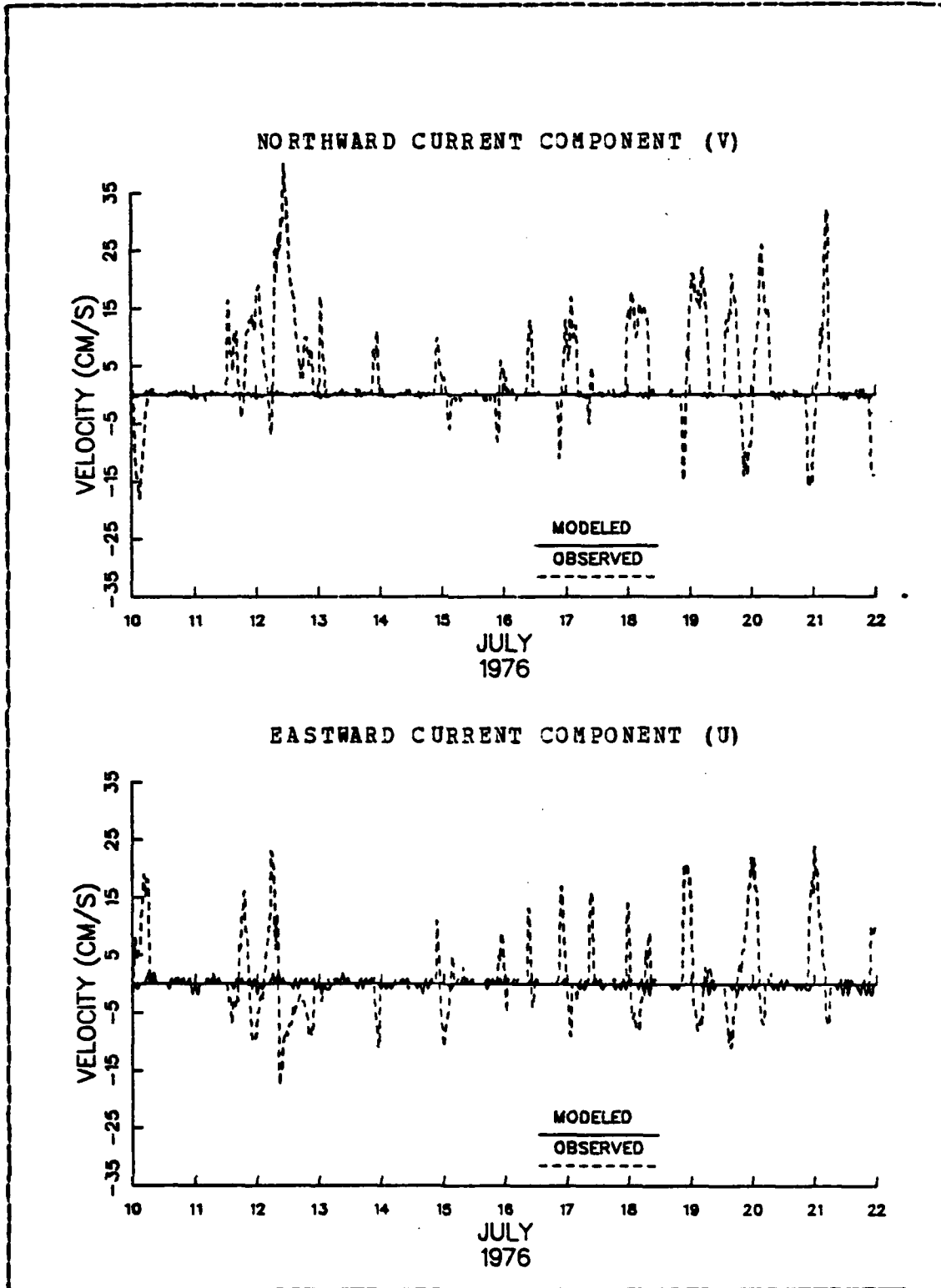


Figure 4.13 Currents North of the Salinas River.

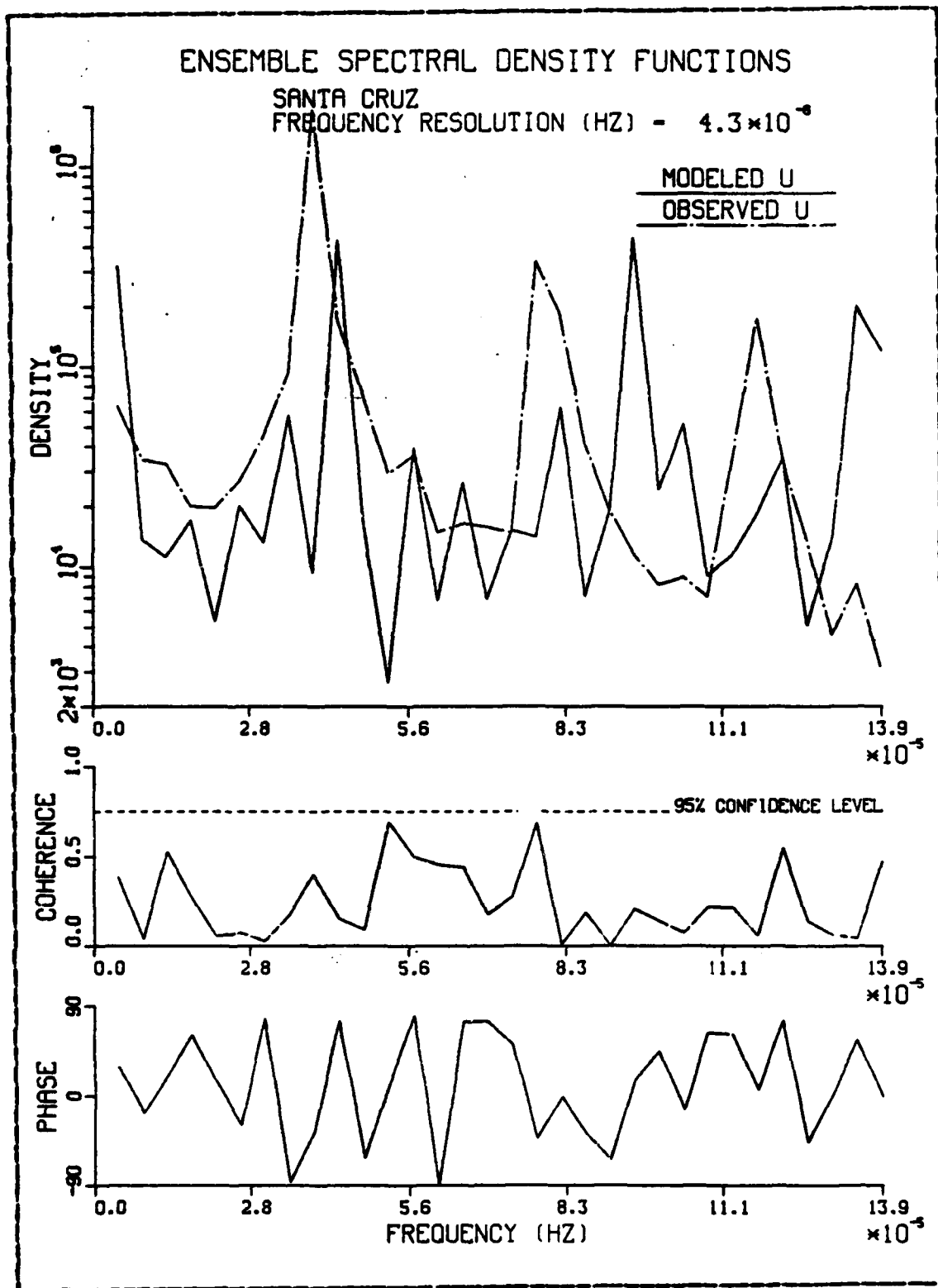


Figure 4.14 Spectra of Currents near Santa Cruz.

The current plots show generally weak (<5 cm/s) tidal flow into and out of the bay, corresponding to periods of flood and ebb. In the southern part of the bay, a strong east-west current (up to 30 cm/s) appears just north of the Monterey peninsula. This jet is consistent with the strong currents experienced by divers in the area.¹ In the northern part of the bay, a broader current (10 cm/s) flows along the depth contours.

Of especial interest is a current pattern that develops between Ano Nuevo and Santa Cruz on current plots made using grid A (Figure 4.15). The gyre, which the model predicts to have speeds ranging from 2 to 10 cm/s, is consistent with the observations of Carter and Kazmierczak (1968) who noted a closed circulation in the area with similar speeds.

2. Tidally Forced Circulation with Wind

When an average wind of 3 m/s (7 mph) from the west-northwest was applied over the entire field of grid B, the tidally forced circulation was unchanged. A maximum wind of 10 m/s (30 mph) from the west-northwest also produced essentially unchanged circulatory patterns. A 12-day series of modeled elevations at Monterey and Moss Landing under the same maximum wind yielded results nearly identical to those without wind.

¹Per conversation with Dr. E. C. Haderlie, Dept. of Oceanography, Naval Postgraduate School, 9/27/83.

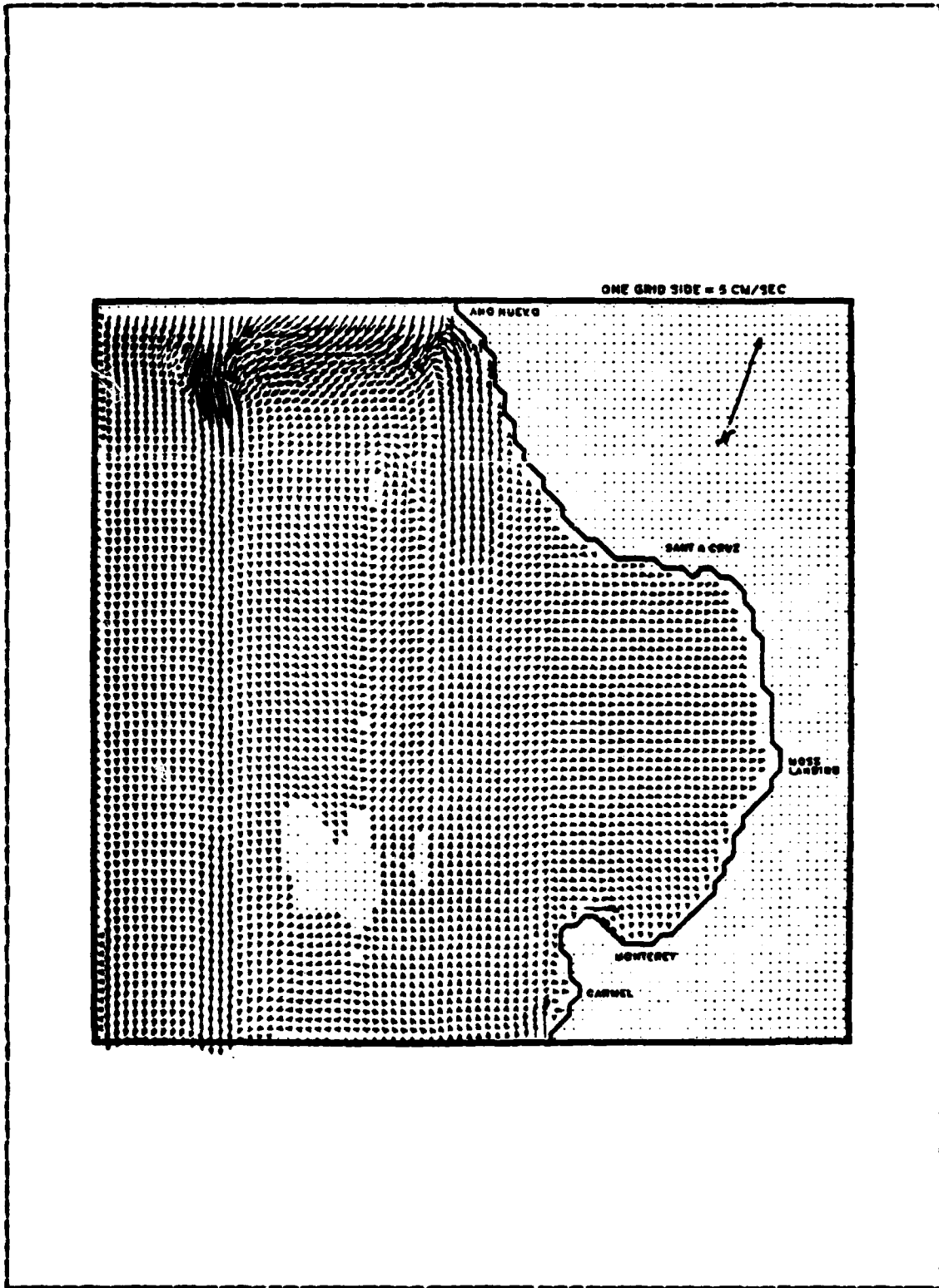


Figure 4.15 Current Field for Grid A at 760702 1500.

V. CONCLUSIONS

A. VALIDITY OF THE MODEL

The numerical model has been shown by comparison with observations to provide reasonably accurate sea-surface elevations. Although the modeled current does not account for the total observed current at comparison stations, it probably accurately reflects the contribution due to the barotropic tide. Much of the remaining observed current may represent response to diurnal wind stress, offshore non-tidal currents, and/or forcing due to internal waves, the last requiring a more complex, three-dimensional model for further investigation. Application of observed winds on a timestep-by-timestep basis might be a fruitful avenue for further investigation.

That numerical instabilities exist in the model has been noted by various authors [Moe, et al., 1978; Benque, et al., 1982], who have proposed some improvements in the model's formulation. The flexibility and accuracy of the model might be improved by further investigation of their suggestions.

B. HYDROGRAPHIC SURVEY APPLICATIONS

A numerical model such as that implemented by this study can improve the process of correcting depths for changes in sea-surface elevation during a hydrographic survey. Advantages of the two-dimensional model over simple extrapolative techniques or more complex, three-dimensional models result from the model's relative simplicity, flexibility, ability to operate in a real-time data collection system, and ability to compute sea-surface elevations with sufficient accuracy.

The tested model is a relatively simple FORTRAN program to implement and use, particularly with the interactive modifications made during this study. It could be further improved in this respect by adding an interrupt/restart routine to permit changes of constants, such as time step or output frequency, during the course of a single computer run. The model is flexible, since it can be readily applied to various coastal areas by means of the gridding software developed during this study.

To implement the model on a microprocessor during data collection in the field, requires the availability of sufficient virtual storage capacity and CPU time to permit unimpeded computations. The virtual storage required depends upon the dimensions of the grid; a more economical use of arrays in the model program can reduce the requirement. In the real-time mode of operation, computations should immediately follow boundary-amplitude updates at each half time step to make efficient use of CPU time. At the conclusion of each full time step the resulting, updated sea-surface elevations are then promptly available.

The time step used depends upon the interval at which water-level observations are available from one or more locations suitable for establishing boundary amplitudes. In the real-time mode, presumably such data could be telemetered to the survey vessel at the standard tide gage frequency of 6 minutes, permitting a model time step of 12 minutes. Since updated elevations can only be available at the conclusion of a time step (Figure 5.1), a 6-minute lag exists that may be removed only by post-survey processing.

Another factor in real-time operation of the model is the start-up time required. The model should be calibrated to establish the validity of friction models and boundary-amplitude algorithms, preferably by comparing the output for several tidal cycles with observed tides at a location in

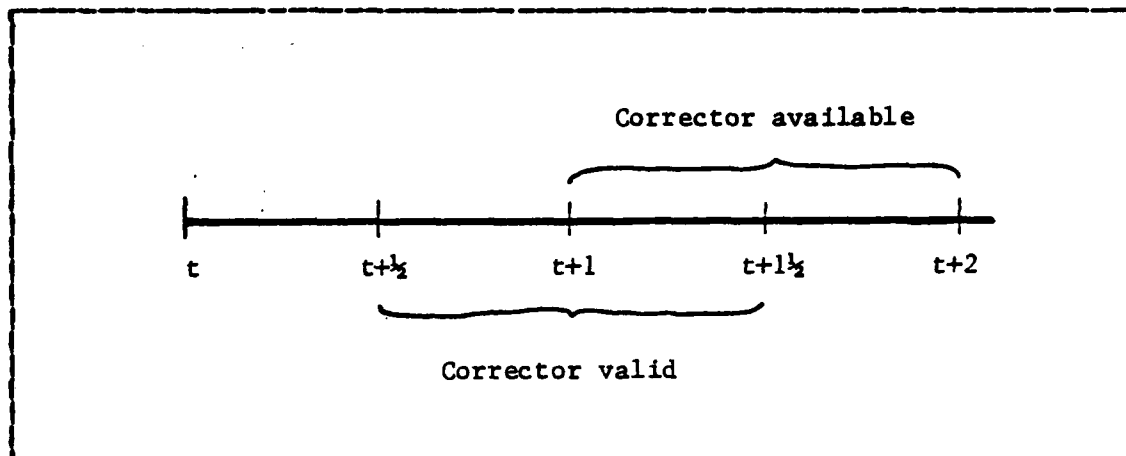


Figure 5.1 Time Step Lag During Real-time Model.

the interior of the survey area. If historical data are not available, this could require several days of observation and analysis prior to the survey.

The accuracy of the model in computing sea-surface elevations from tidal forcing alone has been estimated during this study as 4-8 cm (1 RMS error). Survey requirements are $3\sigma \leq 9.14 + 0.005h$ cm, where σ is the standard error and h is the depth in centimeters [Mobley, 1982]. The depths at the tide gages in this study were about 8 m, permitting a 3σ equal to 13.1 cm. This value was attained at Moss Landing (3 RMS error = 12 cm) and, if the troublesome noise could be removed by post-survey processing of water-level observations to obtain a smooth tidal forcing function, it may be generally attainable.

The model itself requires further development, both in the application to Monterey Bay and in general. Further testing of the application to Monterey Bay should include the introduction of time-varying wind and oceanic currents, as well as forcing at a time step using tidal amplitudes observed at a shorter interval than the 1-hour interval used in this study. The model should also be applied to and

quantitatively tested against other coastal configurations and bathymetries to ensure that sufficient accuracy can be consistently achieved.

APPENDIX A
TIDAL CONSTITUENTS

TIDAL CONSTITUENTS FOR MONTEREY

Monterey Harbor, Municipal Wharf #2, CA
 Station 941-3450
 36°36'30" N 121°53'30" W

	H	k
SM2	1.6280	297.43
SN2	.4250	295.54
SN1	.3660	272.02
SN1	1.2160	97.76
NO1	.0050	164.11
NO1	.7630	81.44
NO1	.0020	306.67
NR3	.0000	.000
SN4	.0030	165.89
SN4	.0030	83.55
NU2	.0690	279.36
NU2	.0030	41.80
NU2	.0460	234.42
NU2	.0460	248.48
OO1	.0390	119.59
LAMBDA2	.0090	281.74
SI1	.0380	202.27
SI1	.1170	114.83
J1	.0710	106.99
SI1	.0150	354.41
SSA	.0300	278.51
SSA	.1460	173.10
SSF	.0160	156.68
SHO1	.0530	180.53
SHO1	.0290	72.73
SHO1	.1370	72.90
SHO1	.0170	271.39
SHO1	.0050	136.85
SHO1	.0190	68.33
SHO1	.3810	92.74
SHO1	.0050	97.96
SHO1	.0100	356.26
SHO1	.0280	285.41
SHO1	.0020	220.13
SHO1	.1210	287.69
SHO1	.0020	143.85
SHO1	.0040	134.56

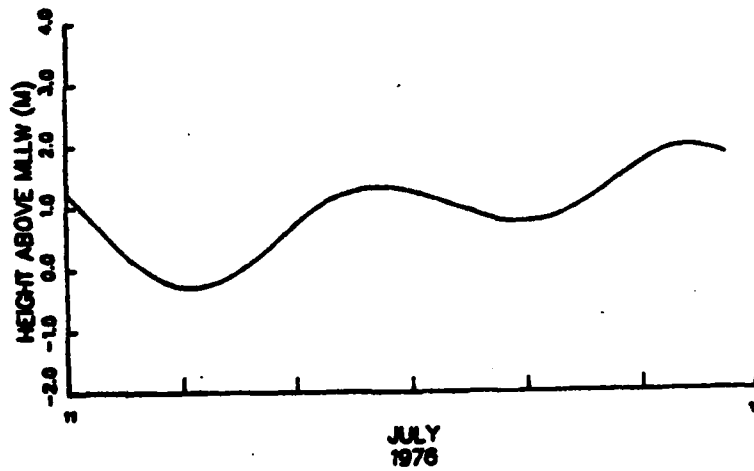
TIDAL CONSTITUENTS FOR MOSS LANDING

Moss Landing, Ocean Pier, CA
 Station 941-3616
 36°48'10 N 121°47'40 W

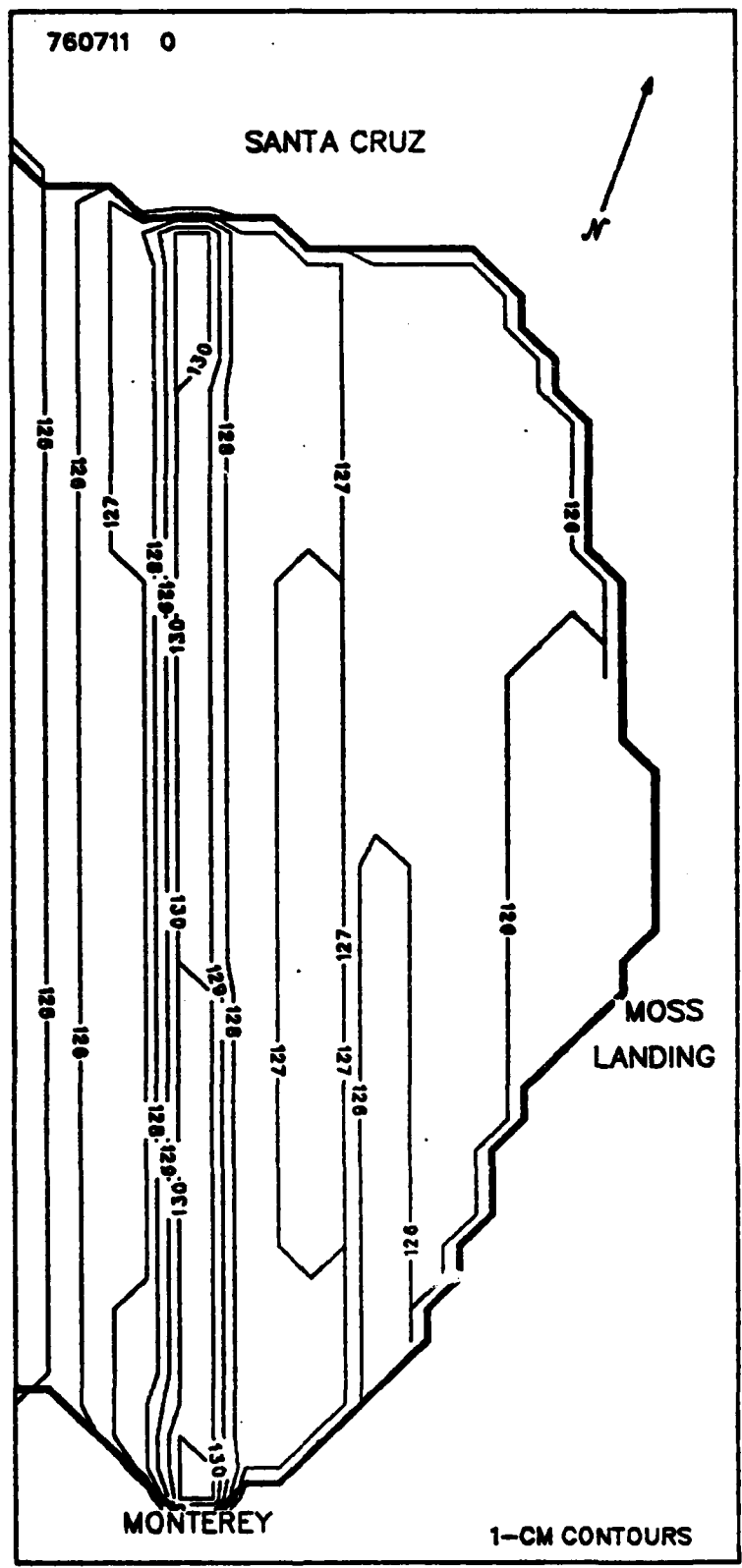
	H	k
M2	1.6636	295.33
S2	.4182	295.84
N2	.3419	269.50
K1	1.1349	99.28
M4	.0178	160.69
O1	.7278	81.83
M6	.0172	63.79
MK3	.0000	.00
S4	.0064	141.43
MN4	.0000	.00
MU2	.0663	272.96
S6	.0047	194.21
MU2	.0000	.00
2N2	.0455	243.67
OO1	.0313	116.72
LAMBDA2	.0116	295.57
S1	.0000	.00
M1	.0517	90.55
J1	.0575	108.00
MH	.0000	.00
SSA	.0000	.00
SSA	.0000	.00
MSF	.0000	.00
MP	.0000	.00
RHO1	.0277	74.33
O1	.1412	73.11
M2	.0247	295.84
M2	.0033	295.84
2O1	.0189	64.39
PT	.3757	99.28
SM2	.0000	.00
M3	.0000	.00
L2	.0466	321.16
MK3	.0000	.00
K2	.1137	295.84
M8	.0110	336.89
MS4	.0000	.00

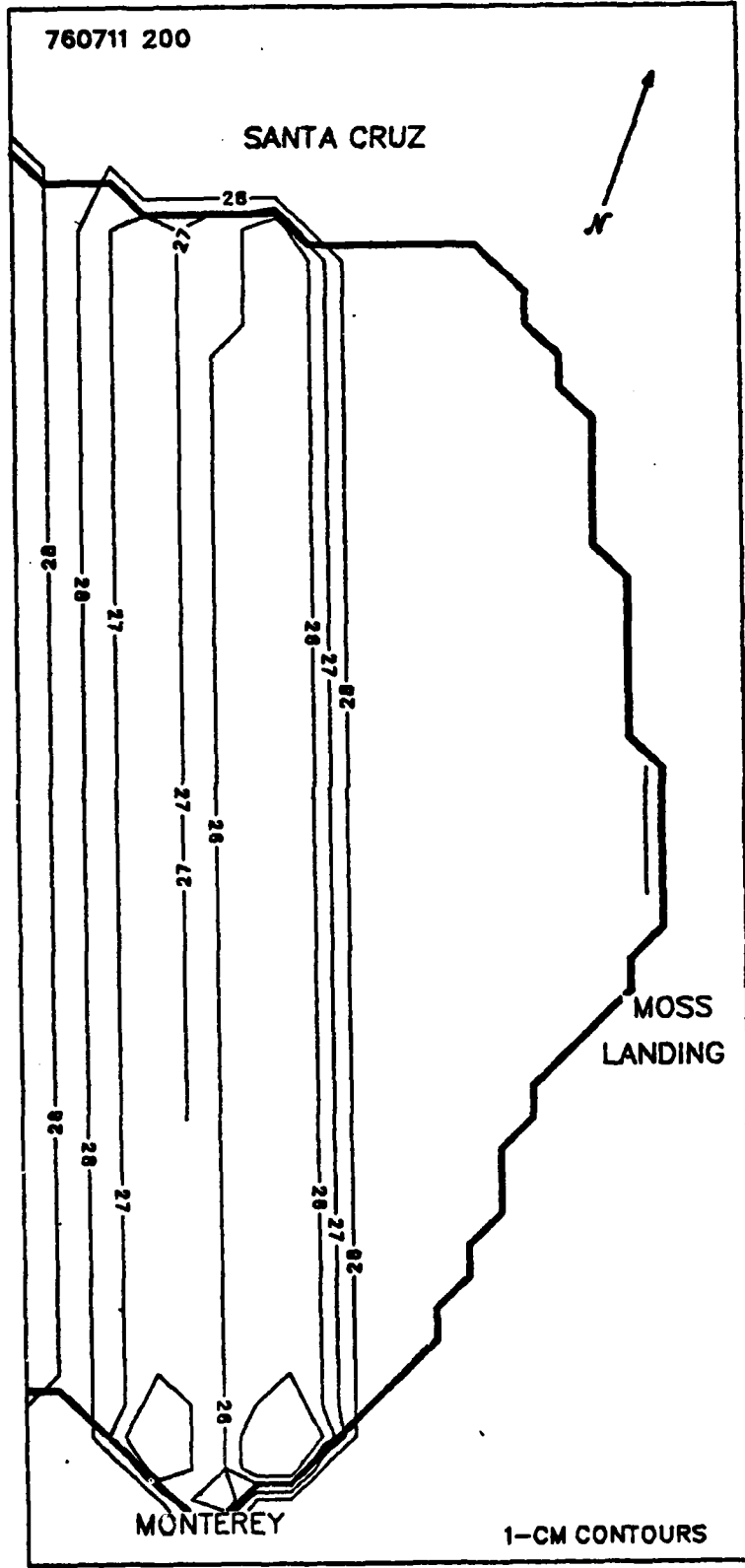
APPENDIX B
TIDALLY FORCED SEA-SURFACE ELEVATIONS

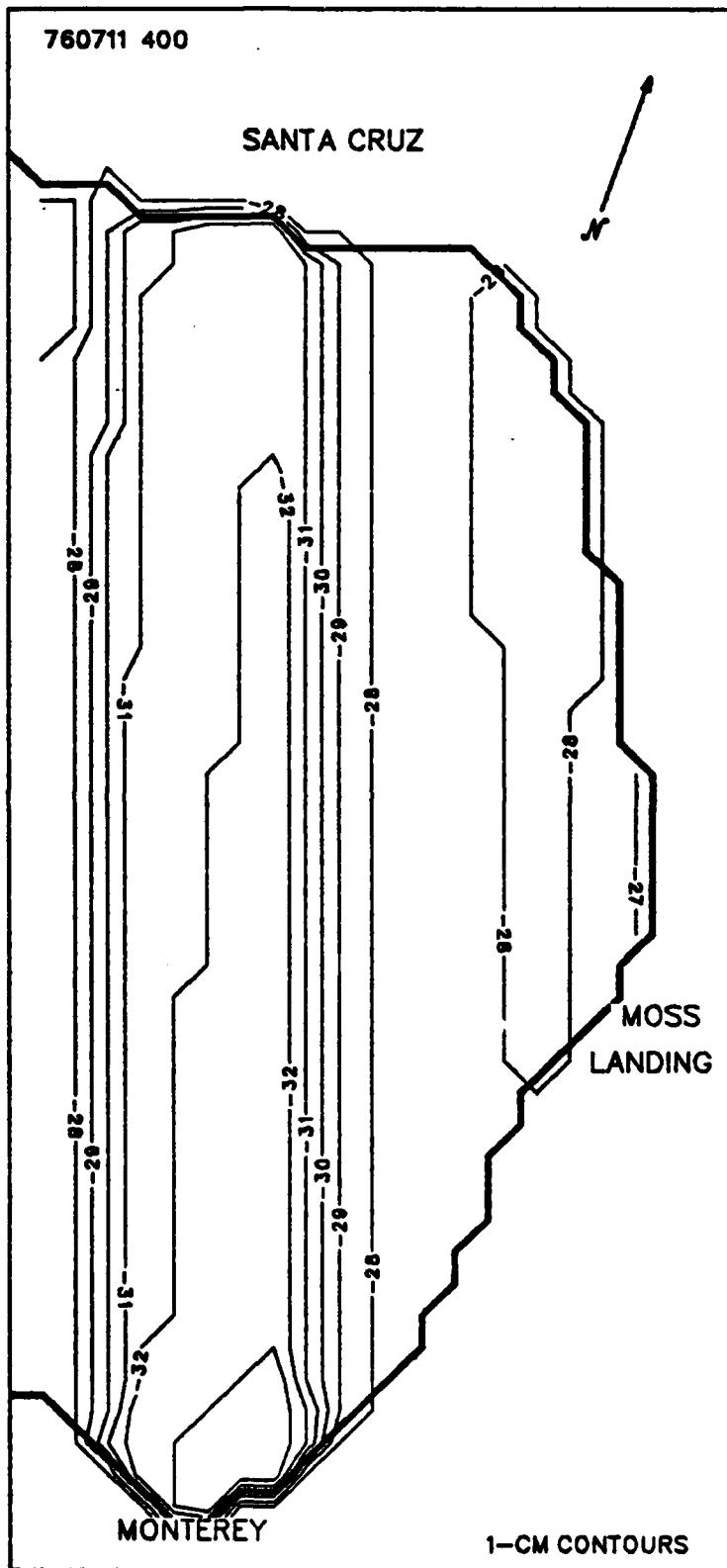
SEA-SURFACE ELEVATIONS AT MONTEREY

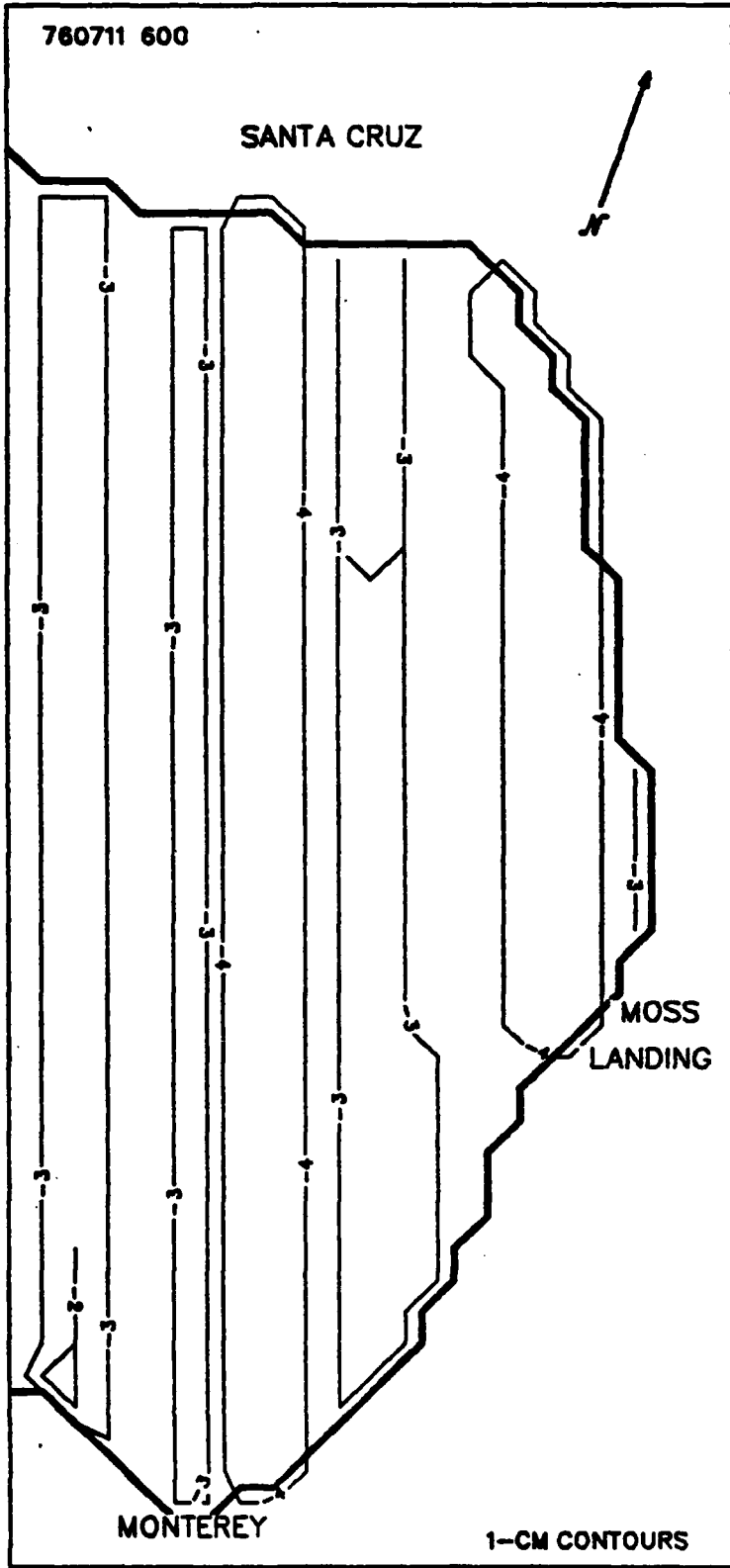


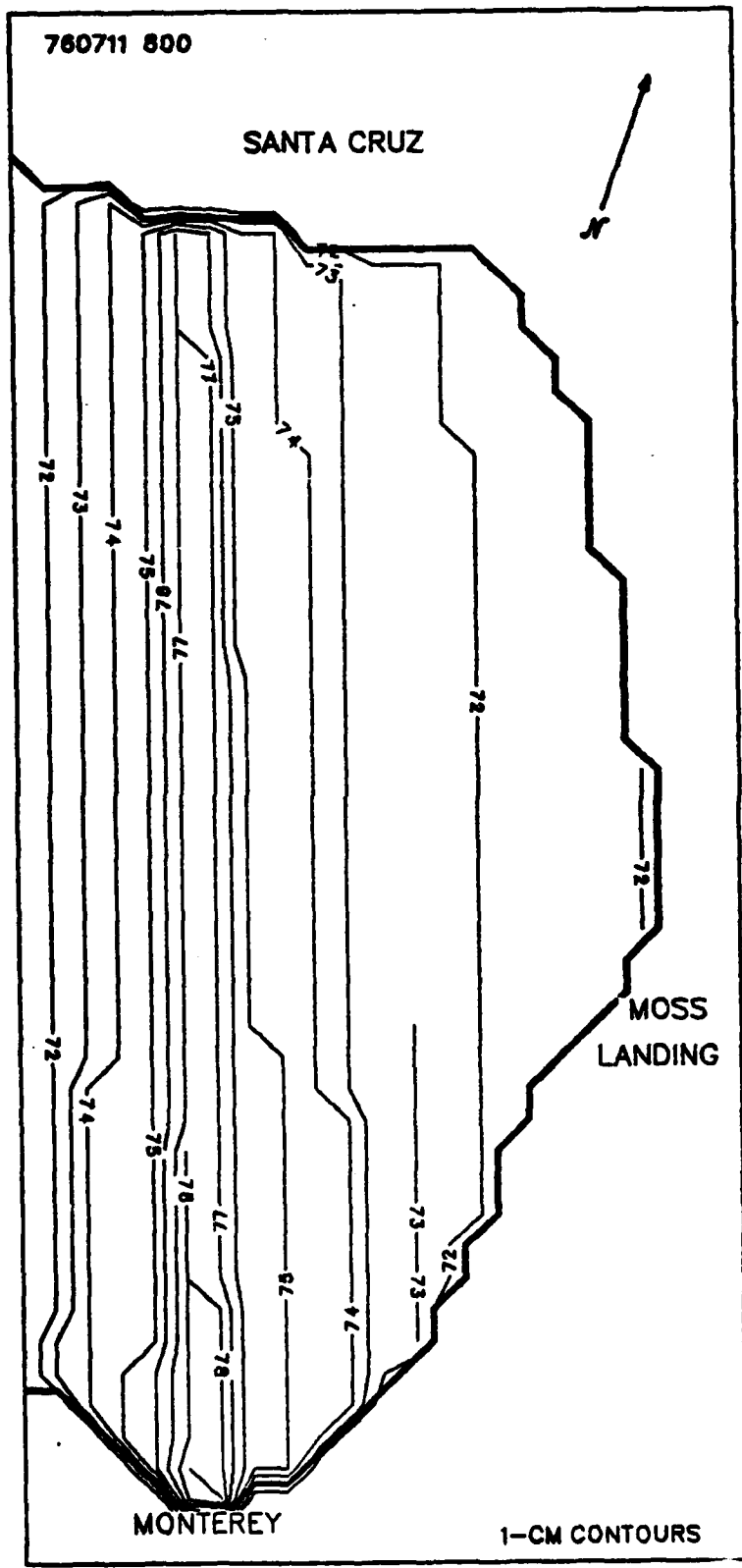
Tidal cycle for the following
2-hour time series.

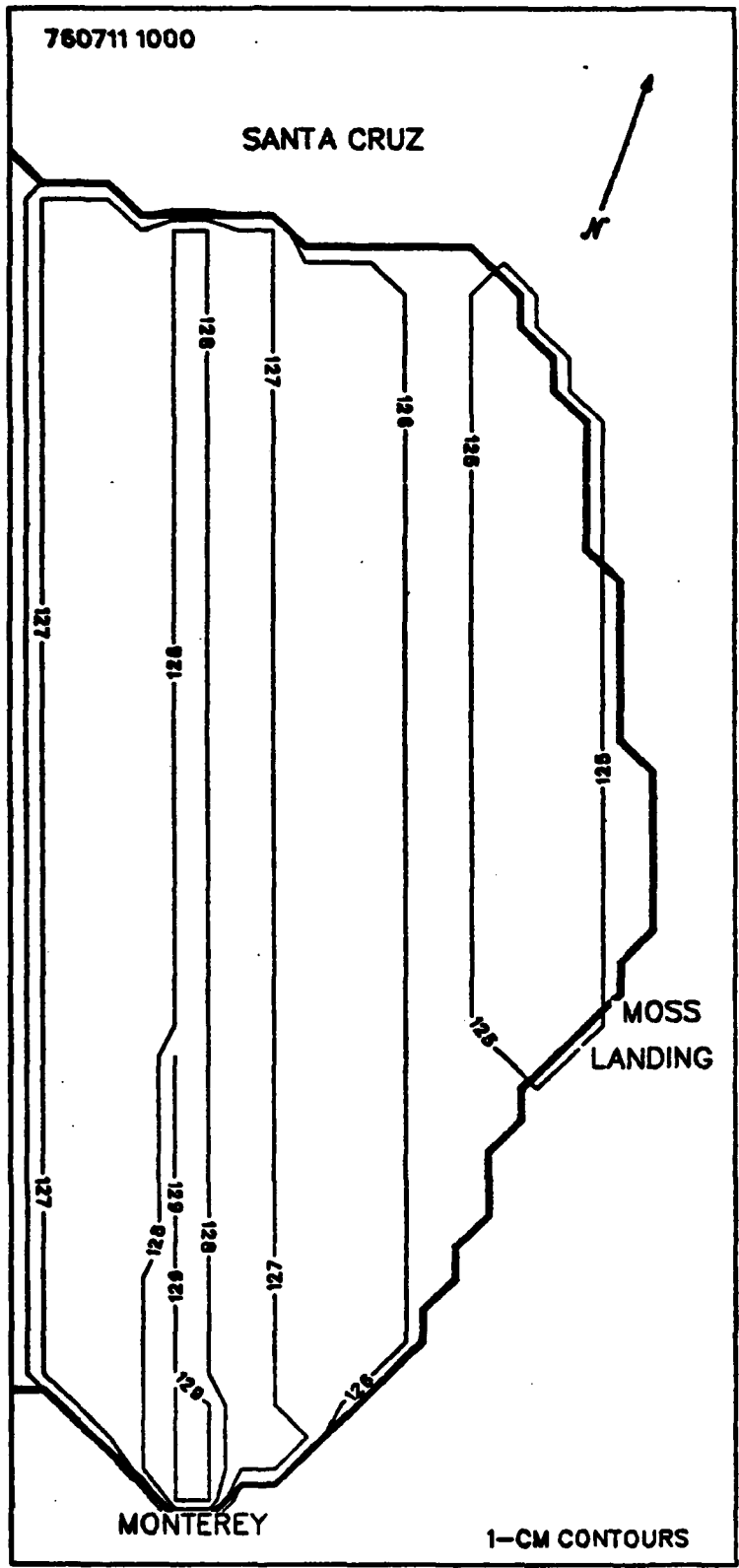


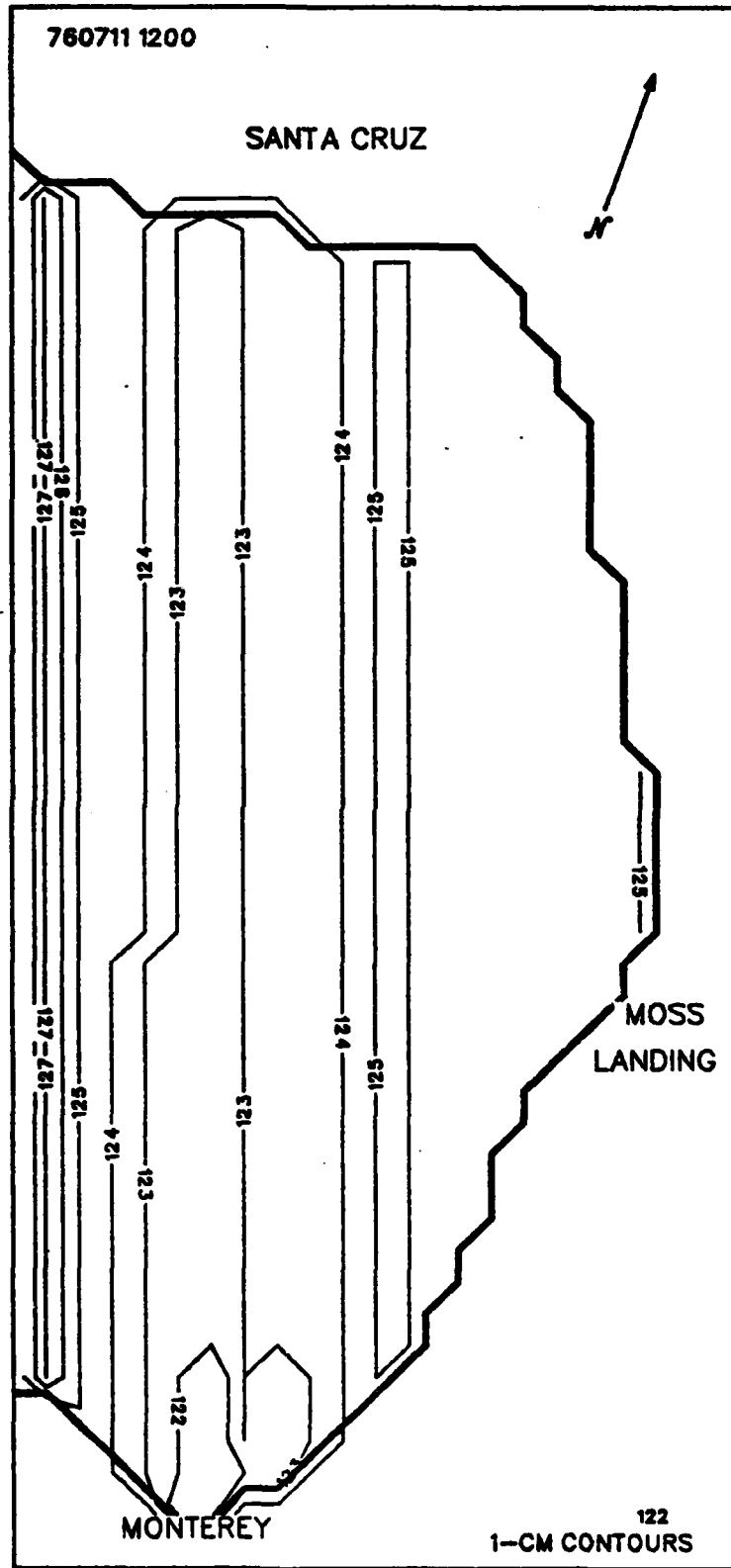


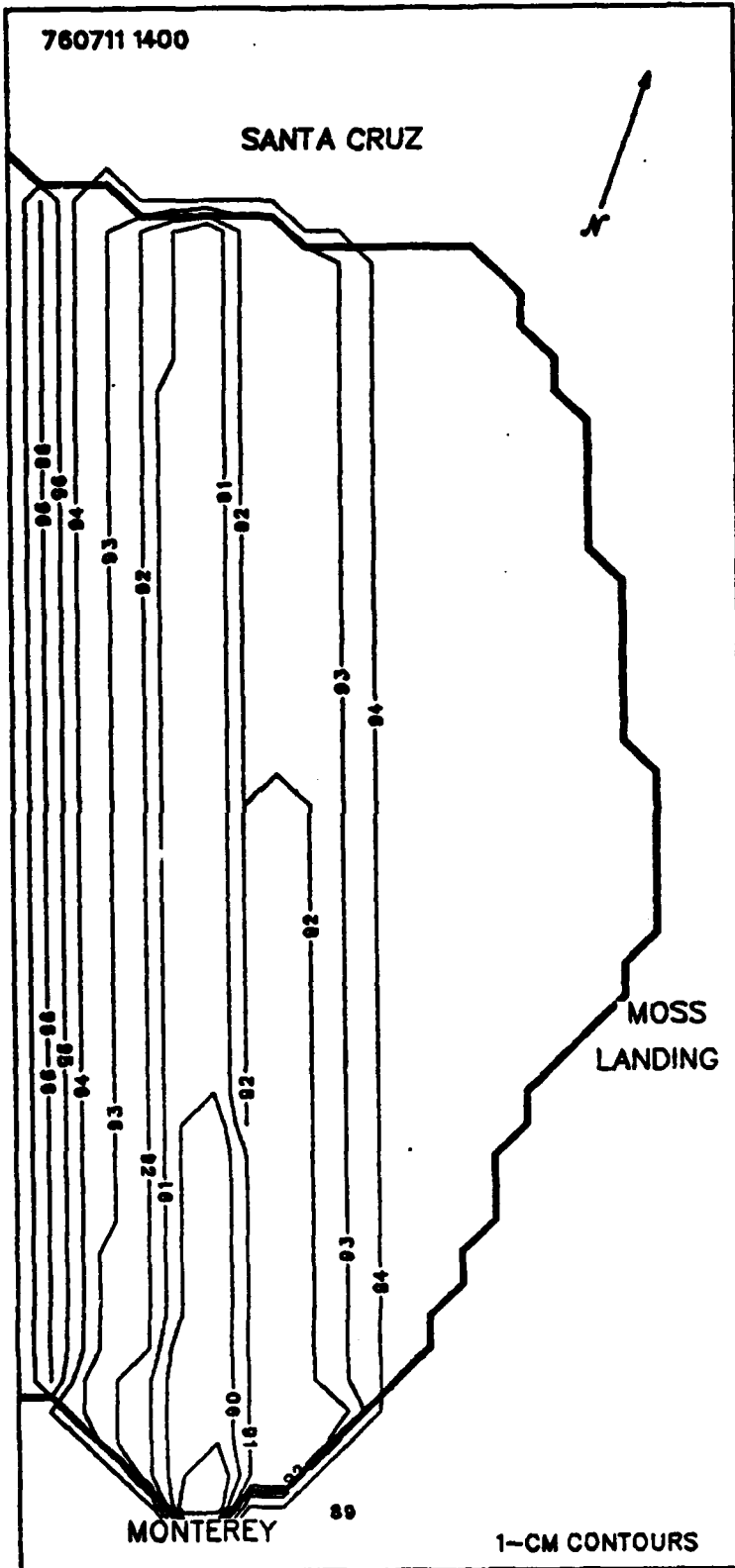


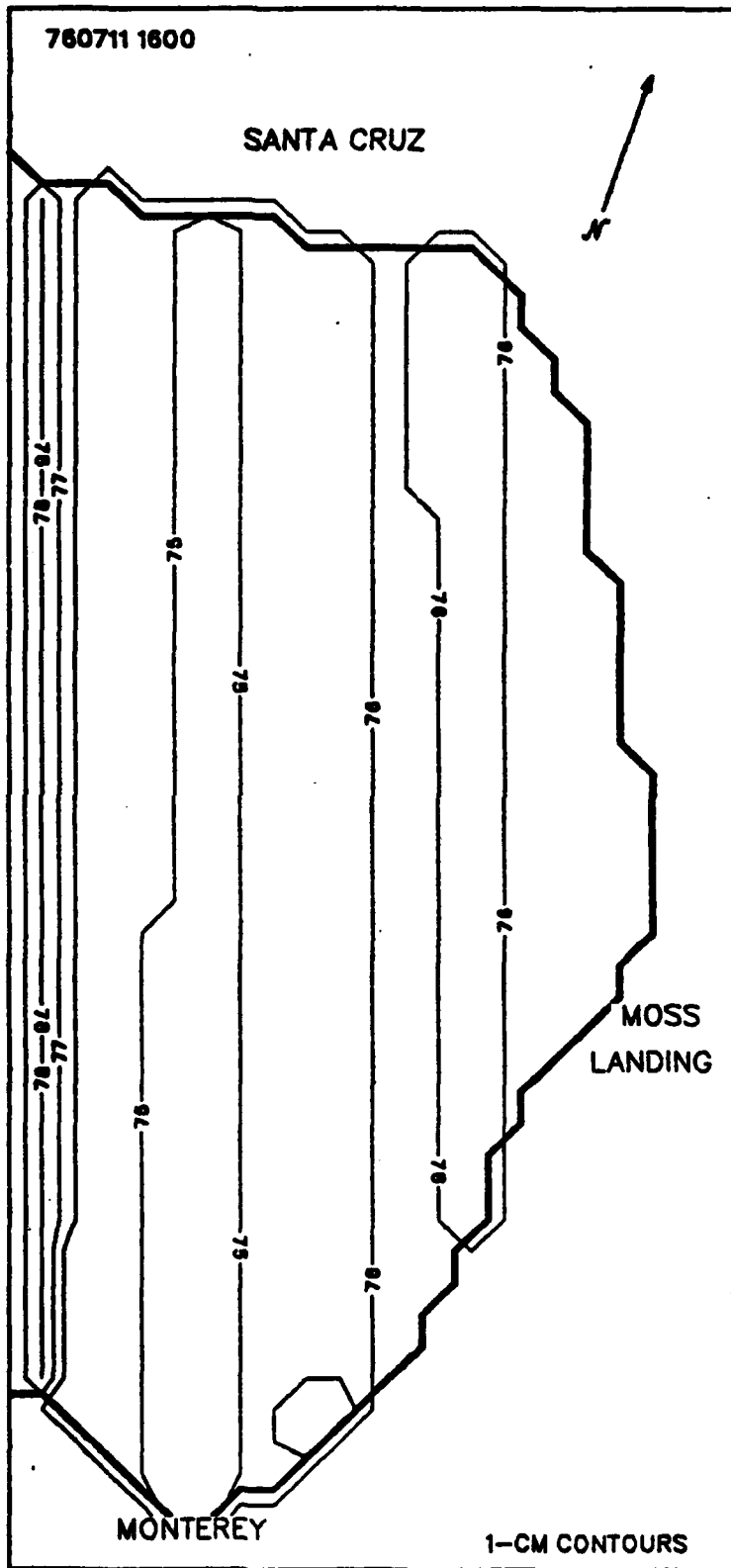


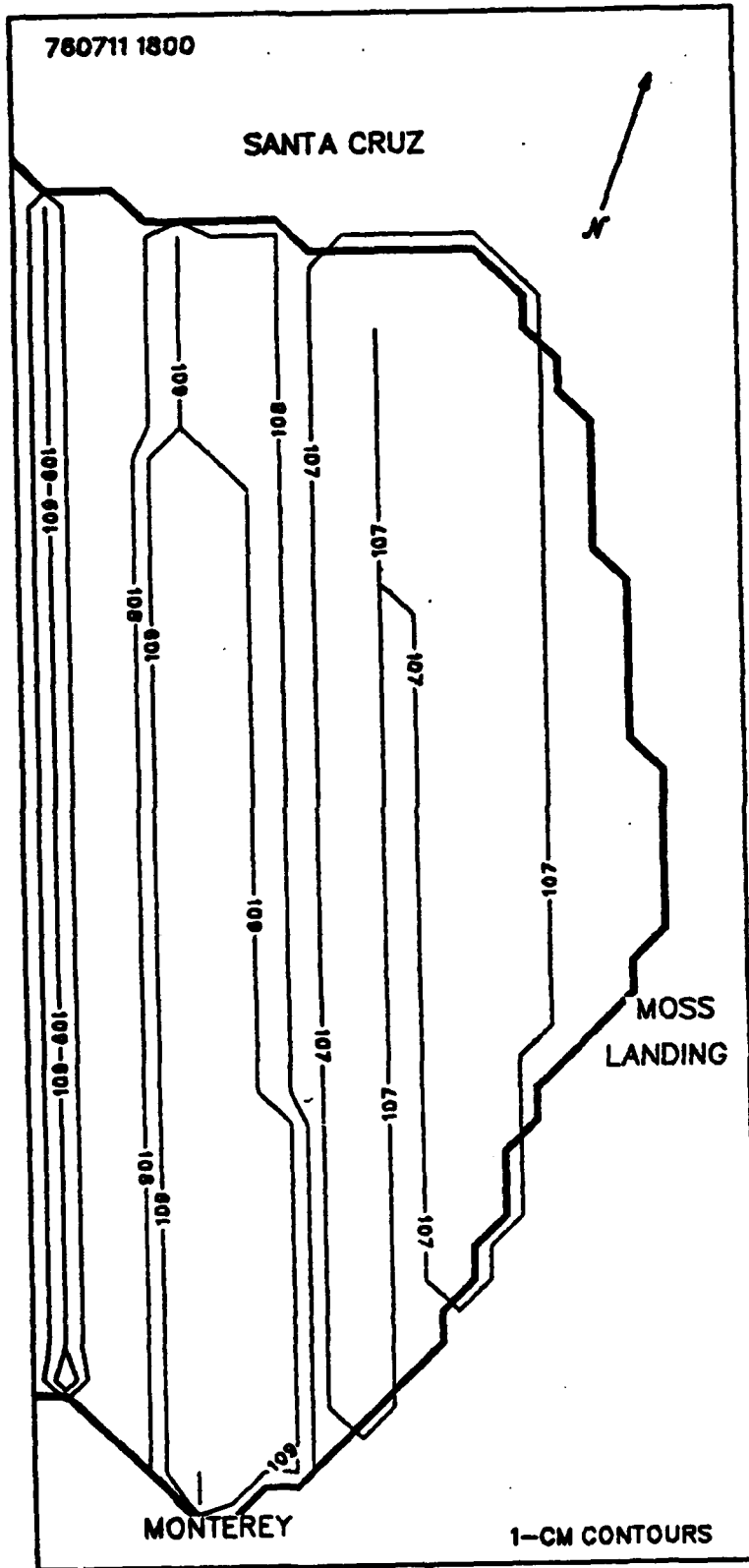


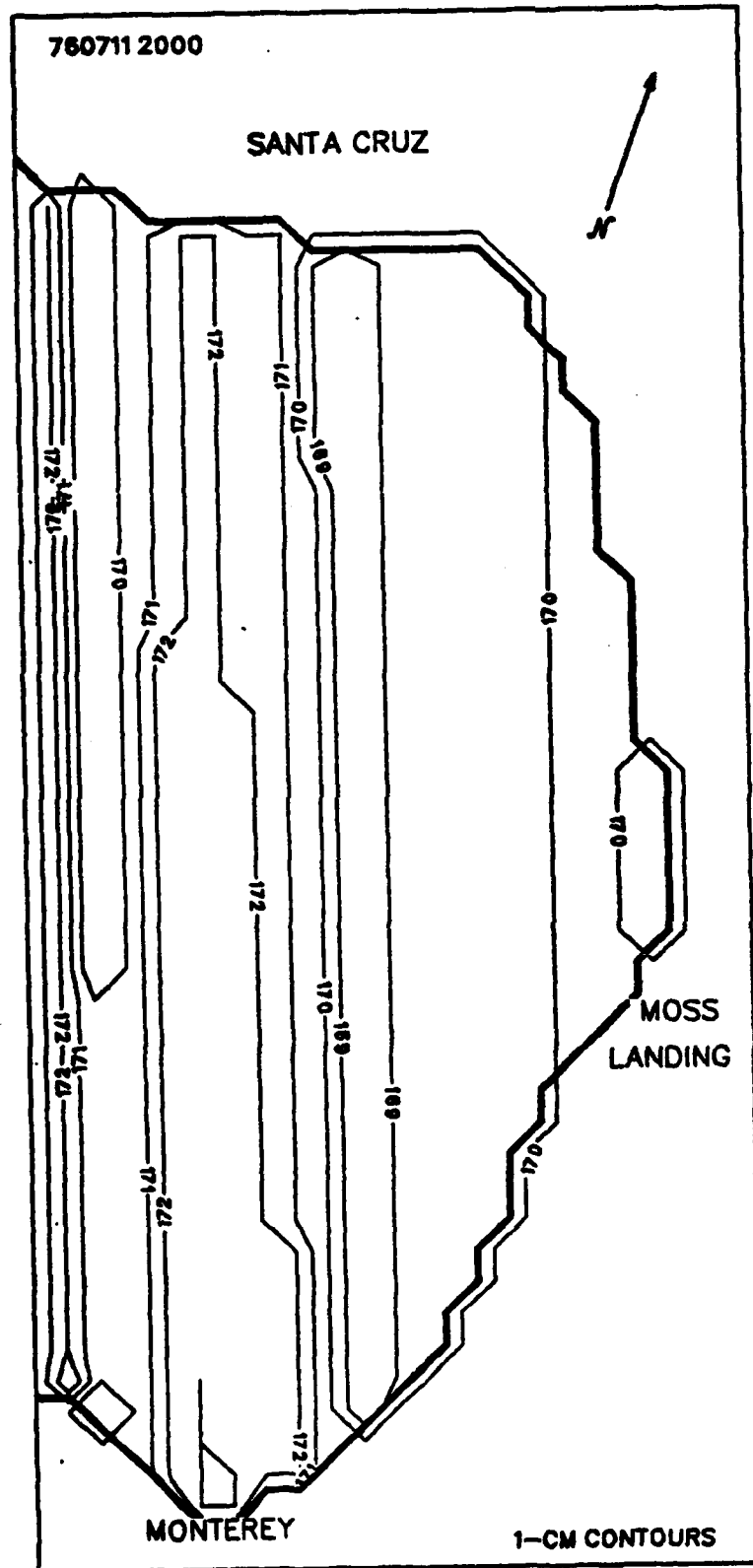






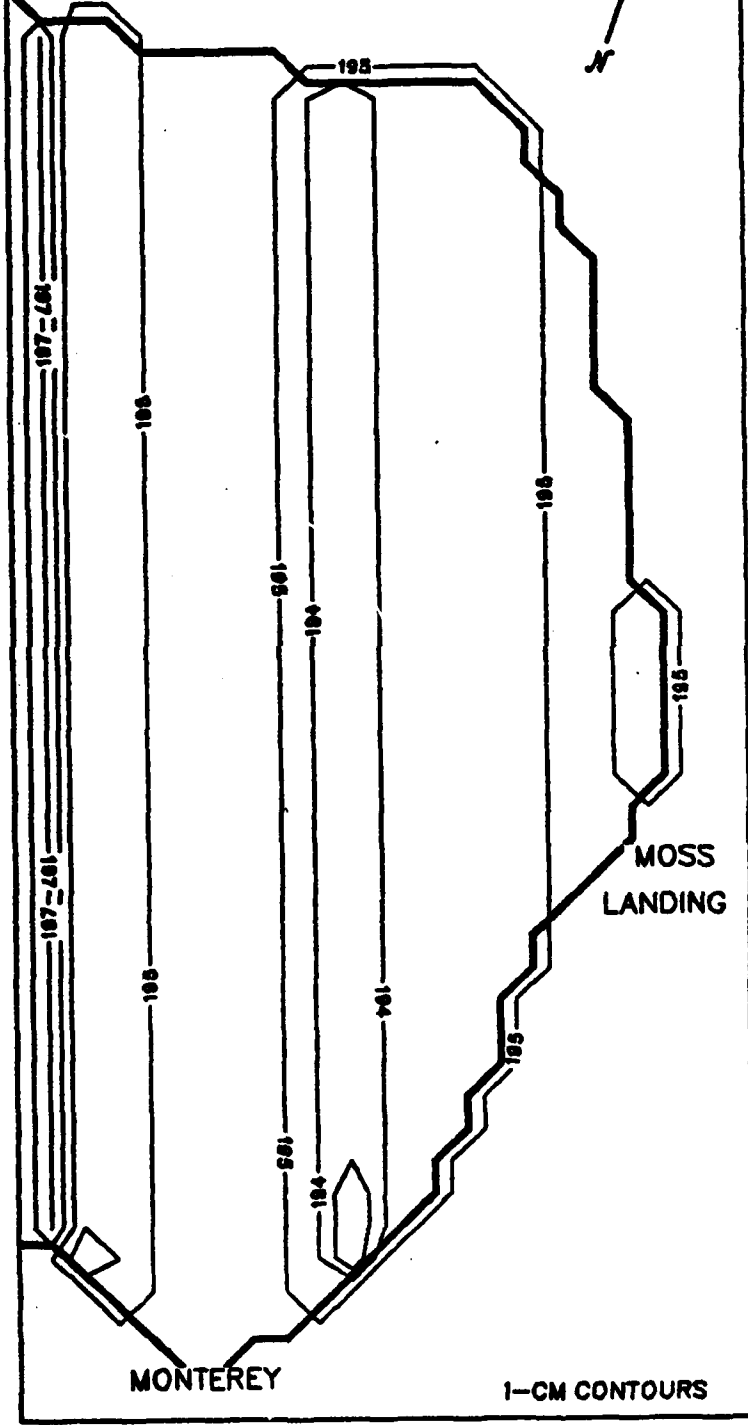






760711 2200

SANTA CRUZ



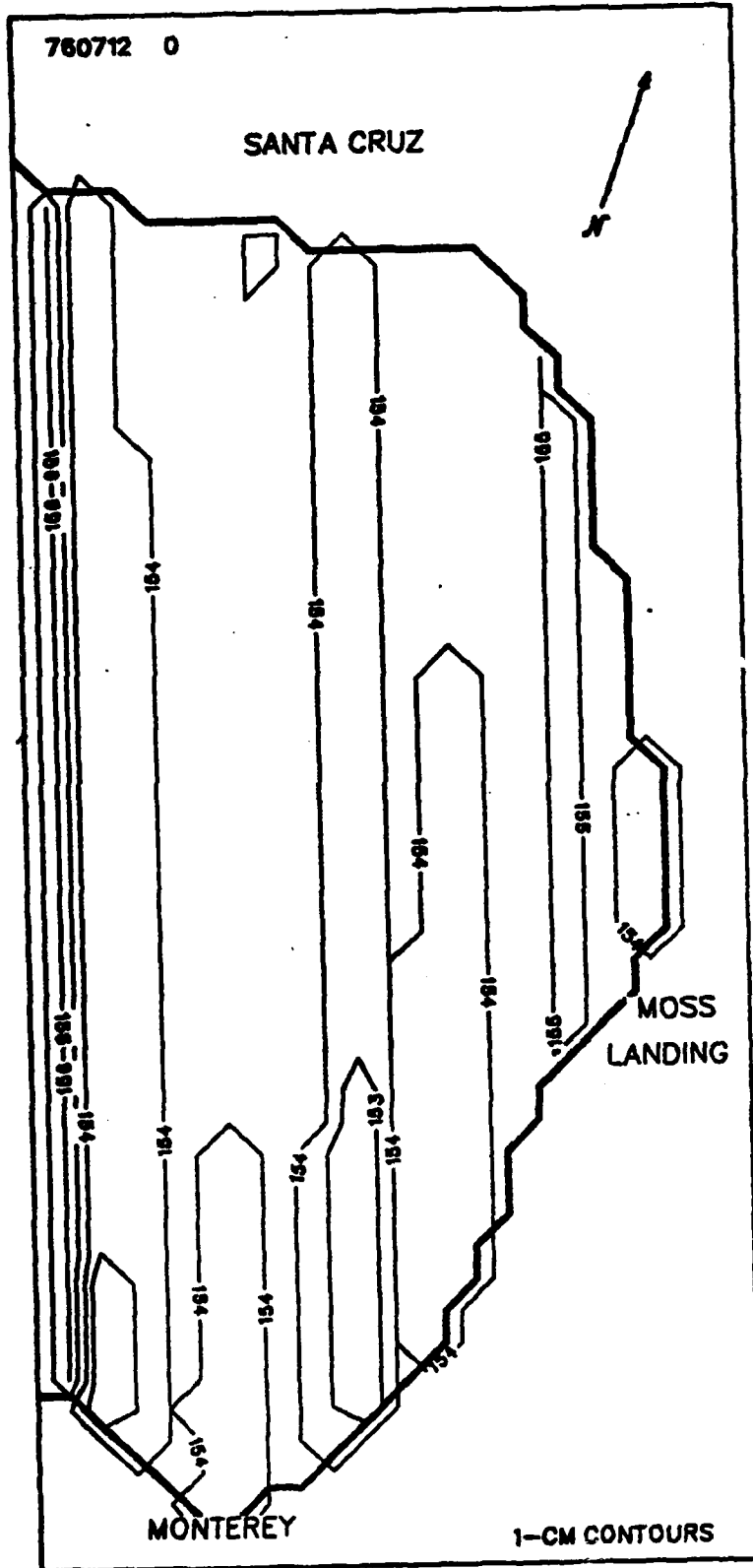
MONTEREY

MOSS
LANDING

1-CM CONTOURS

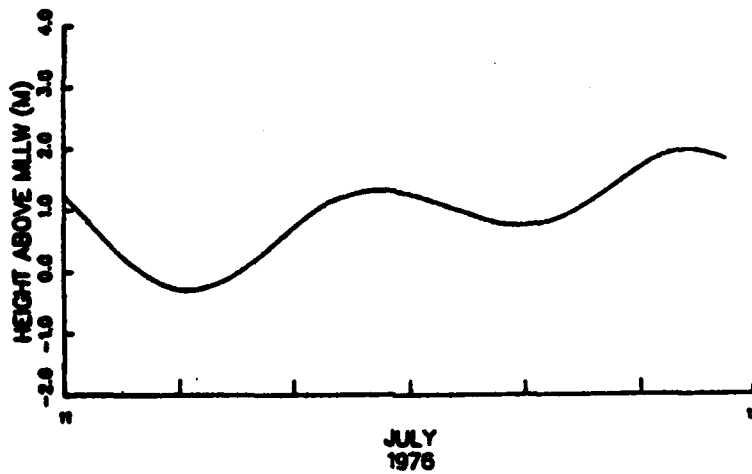
760712 0

SANTA CRUZ



APPENDIX C
TIDALLY FORCED CURRENTS

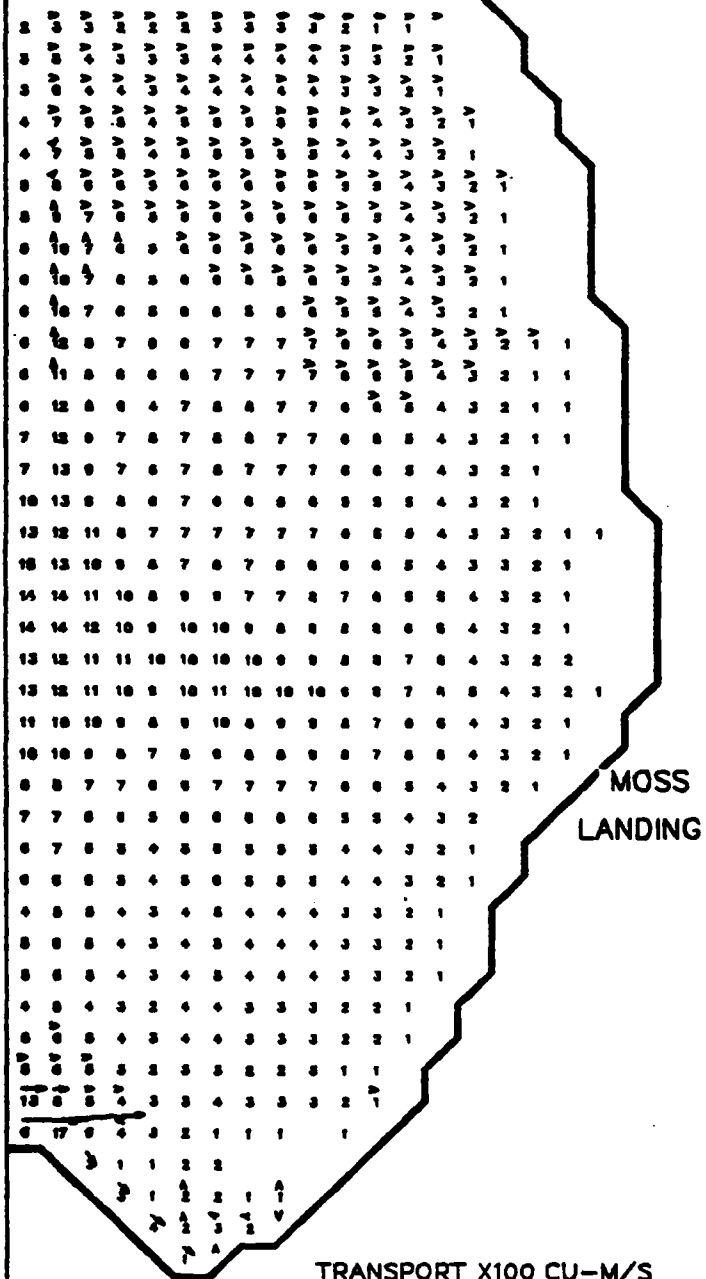
SEA-SURFACE ELEVATIONS AT MONTEREY



Tidal cycle for the following
2-hour time series.

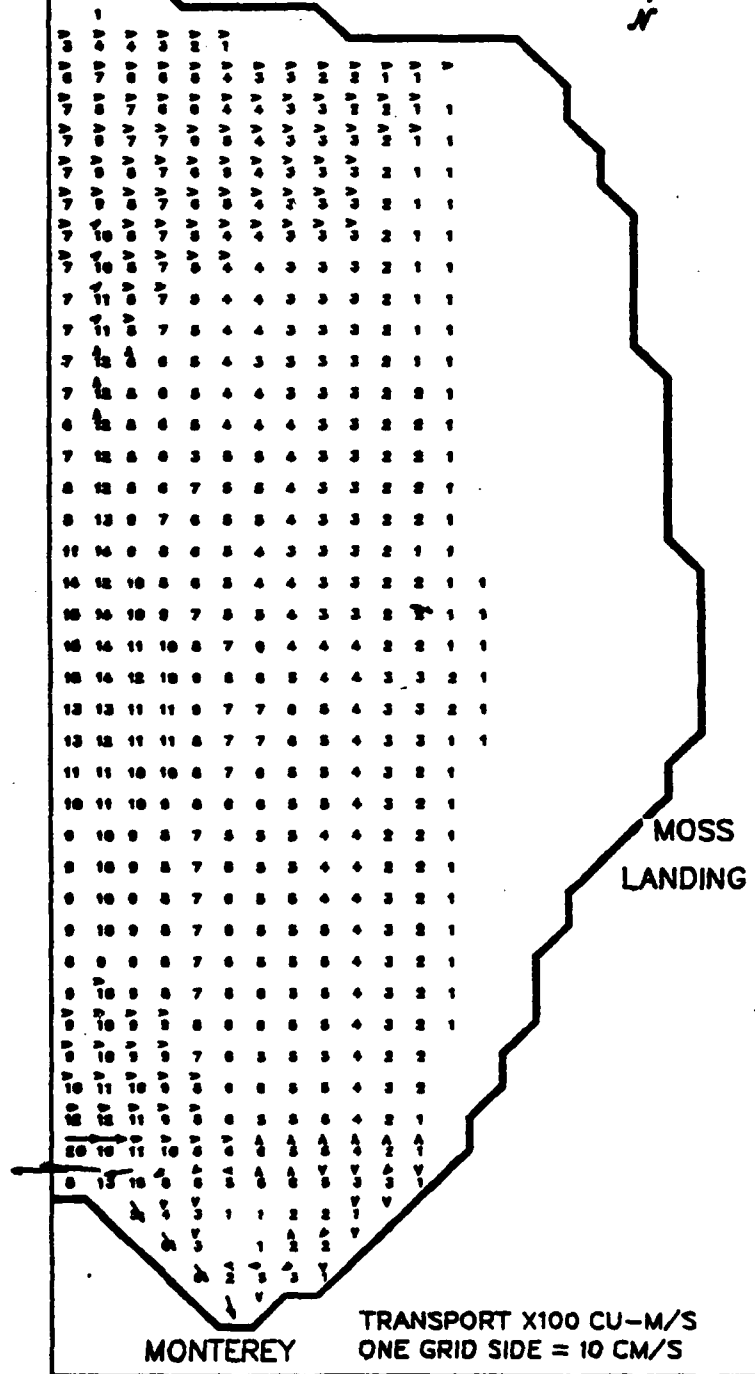
760711 600

SANTA CRUZ



760711 1000

SANTA CRUZ

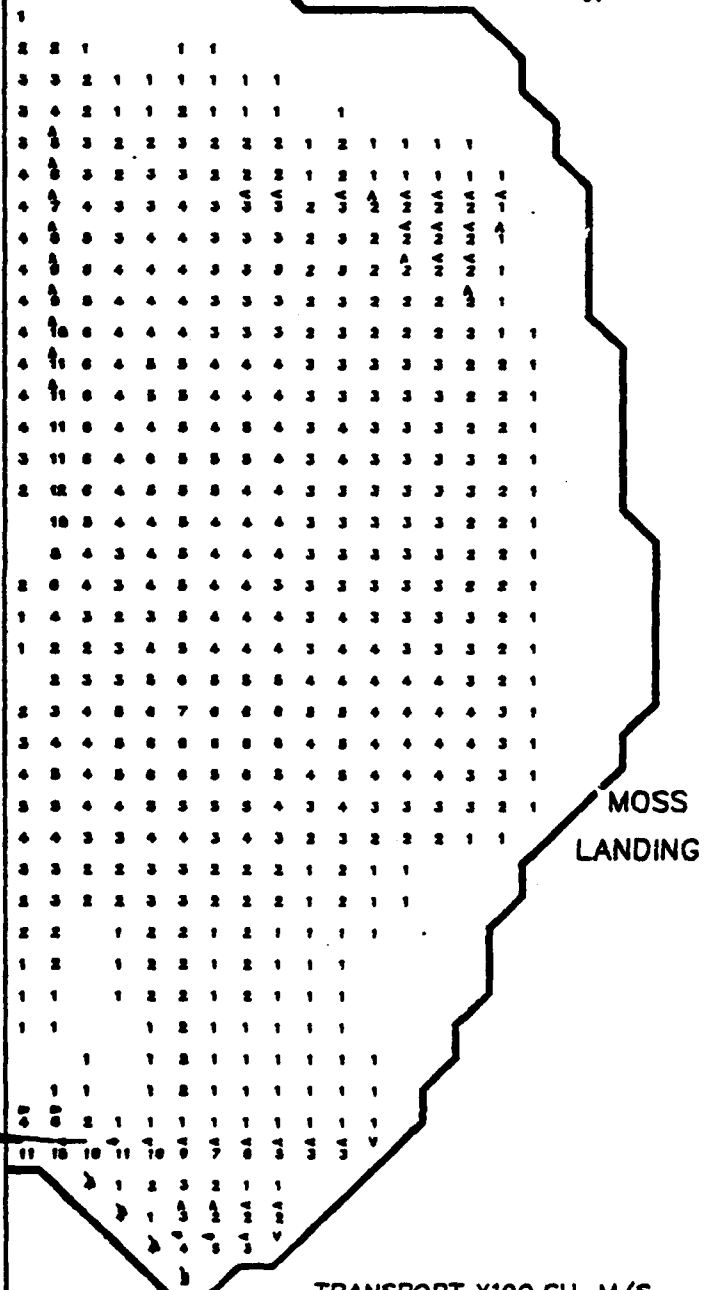


MONTEREY

TRANSPORT X100 CU-M/S
ONE GRID SIDE = 10 CM/S

760711 1200

SANTA CRUZ

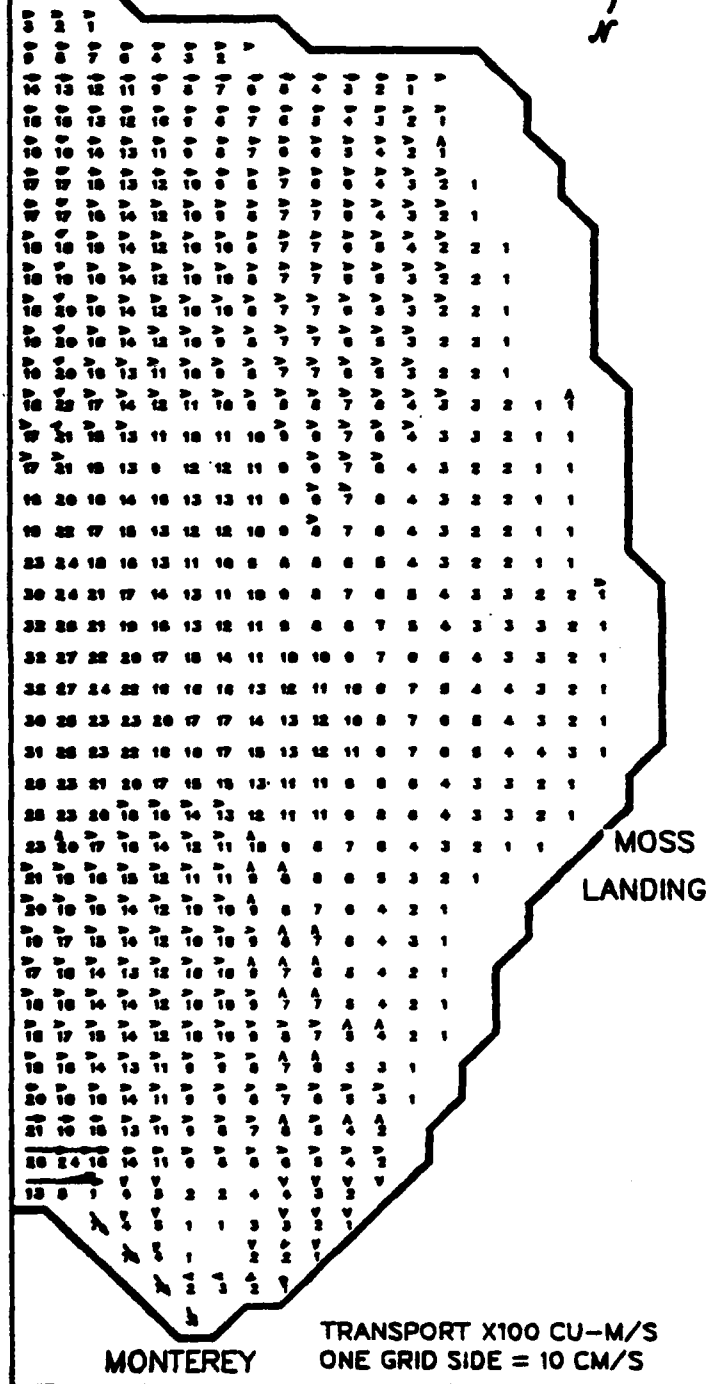


MONTEREY

TRANSPORT X100 CU-M/S
ONE GRID SIDE = 10 CM/S

760711 2000

SANTA CRUZ

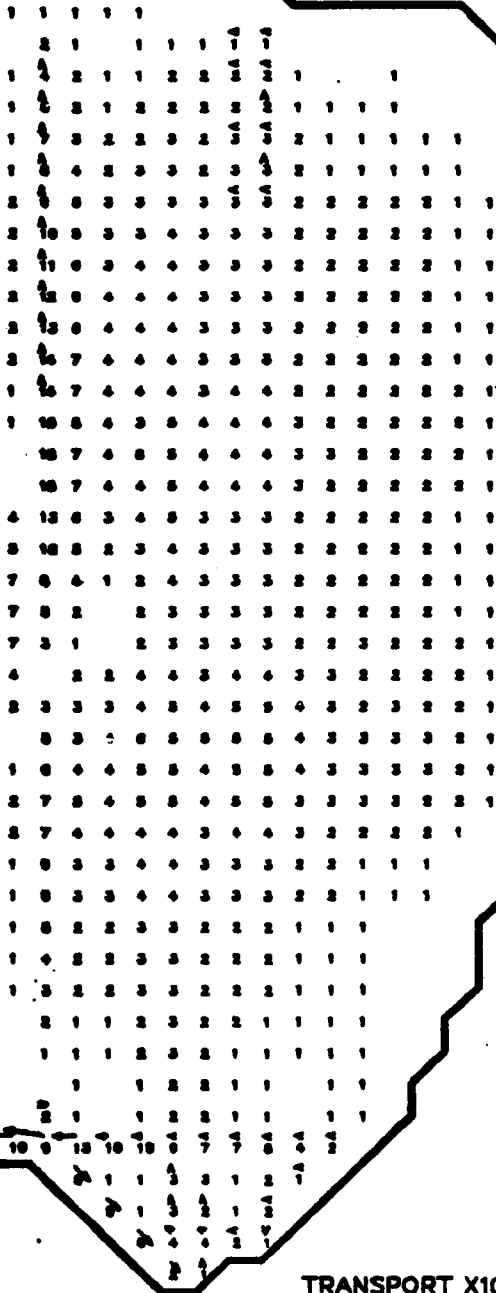


MONTEREY

TRANSPORT X100 CU-M/S
ONE GRID SIDE = 10 CM/S

760711 2200

SANTA CRUZ



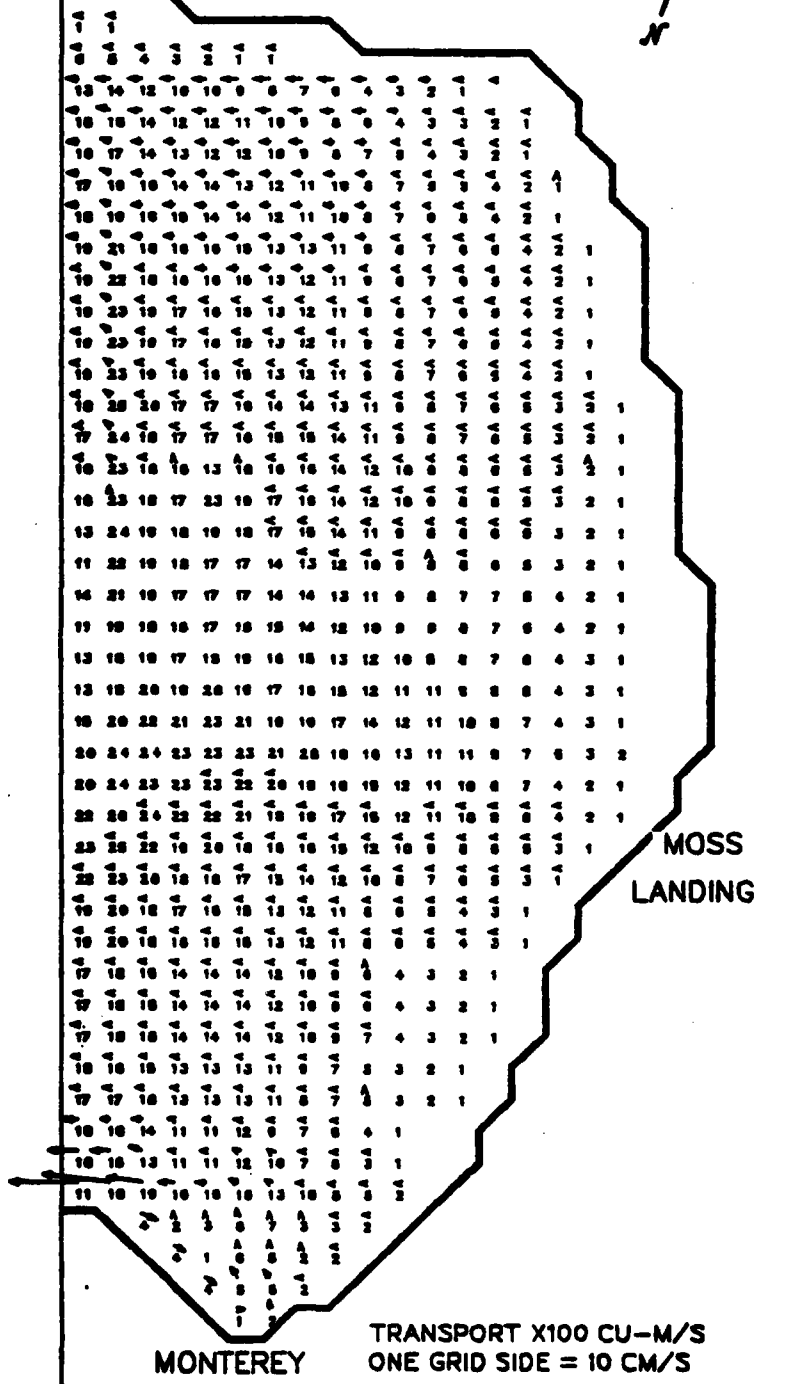
MOSS
LANDING

MONTEREY

TRANSPORT X100 CU-M/S
ONE GRID SIDE = 10 CM/S

760712 0

SANTA CRUZ



BIBLIOGRAPHY

- Benque, J. P., and others, "New Method for Tidal Current Computation," ASCE Journal of the Waterway, Port, Coastal and Ocean Division, v. 108, pp. 396-417, August, 1982.
- Bretschneider, D. E., Sea Level Variations at Monterey, California, M.Sc. Thesis, Naval Postgraduate School, 1980.
- Broenkow, W. W. and Smetlie, W. M., Jr., "Surface Circulation and Replacement of Water in Monterey Bay," Estuarine and Coastal Marine Science, v. 6, pp. 583-603, 1978.
- Brown and Caldwell, Inc., Oceanographic Predesign Phase Report, Santa Cruz Wastewater Facilities Planning Study, 1978.
- Carter, R. C. and Kazmierczak, E. J., Special Oceanographic Studies, San Francisco Bay-Delta Quality Control Program, Engineering-Science, Inc. Final Report, Task VII-1a, 1968.
- Cartwright, D. E., Zetler, B. D., and Hamon, B. V., Pelagic Tidal Constants, IUGG/IAPSO Publication Scientifique No. 30, 1979.
- Chiang, W. C. and Lee, J. J., "Simulation of Large-scale Circulation in Harbors," ASCE Journal of the Waterway, Port, Coastal and Ocean Division, v. 108, pp. 17-31, February, 1982.
- Clarke, A. J. and Battisti, D. S., "The Effect of Continental Shelves on Tides," Deep-Sea Research, v. 28A, pp. 665-682, 1981.
- Csanady, G. T., Circulation in the Coastal Ocean, D. Reidel, 1982.
- Dronkers, J. J., Tidal Computations in Rivers and Coastal Waters, North-Holland, 1964.
- Engineering-Science, Inc., Oceanographic Investigations in Central Monterey Bay, Survey Activities July 1976 - March 1977, 1977.
- Environmental Research Consultants, Inc., Watsonville Wastewater Treatment Facility Design Project, Predesign and Preliminary Ocean Study: Final Report, Vol. 1, Oceanography, 1976.

- Garcia, R. A., Numerical Simulation of Currents in Monterey Bay, M.Sc. Thesis, Naval Postgraduate School, 1977.
- Gill, S. K. and Porter, D. L., "Theoretical Offshore Tide Range Derived from a Simple Defant Tidal Model," International Hydrographic Review, v. 57, pp. 155-167, January, 1980.
- Hart, W. E., A Numerical Study of Currents, Circulation and Surface Elevations in Chandeleur-Breton Sounds, Louisiana, Ph.D. Thesis, Louisiana State University, 1976.
- Henderson, F. M., Open Channel Flow, Macmillan, 1966.
- Lazanoff, S. M., An Evaluation of a Numerical Water Elevation and Tidal Current Prediction Model Applied to Monterey Bay, M.Sc. Thesis, Naval Postgraduate School, 1977.
- Leendertse, J. J., Aspects of a Computational Model for Long-period Water-wave Propagation, The Rand Corporation MR-5294-PR, 1967.
- Leendertse, J. J., and Liu, S. K., A Water-Quality Simulation Model for Well Mixed Estuaries and Coastal Seas; Vol. VII: A Hindcast, The Rand Corporation R-1774-NYC, 1975.
- Luther, D. and Wunsch, C., "Tidal Charts of the Central Pacific Ocean," Journal of Physical Oceanography, v. 5, pp. 222-230, 1975.
- Lynch, T. J., Long Wave Study of Monterey Bay, M.Sc. Thesis, Naval Postgraduate School, 1970.
- Mobley, W. L., Item 10. in U.S. Dept. of Commerce, NOAA, Charting and Geodetic Service letter: C. W. Hayes N/CG2 to J. S. Higgely N/CGx2, Subject: Hydrographic Thesis Topics for the Naval Postgraduate School, January 6, 1983.
- Moe, J., Mathisen, J. P., and Hodgins, S., "An Improved Method for the Computation of Shallow Water Waves," Numerical Methods in Laminar and Turbulent Flow, pp. 609-618, Pentech press, 1978.
- Munk, W., Snodgrass, F., and Wimbush, M., "Tides Offshore: Transition from California to Deep Sea Waters," Geophysical Fluid Dynamics, v. 1, pp. 161-235, 1970.
- National Geophysical Data Center, U.S. Dept. of Commerce, NOAA, Digital Bathymetric Data for the U.S. Coastal Regions.

AD-A135 077

A MODEL FOR TIDAL CIRCULATION ADAPTED TO MONTEREY BAY
CALIFORNIA(U) NAVAL POSTGRADUATE SCHOOL MONTEREY CA
C W SCHOMAKER SEP 83

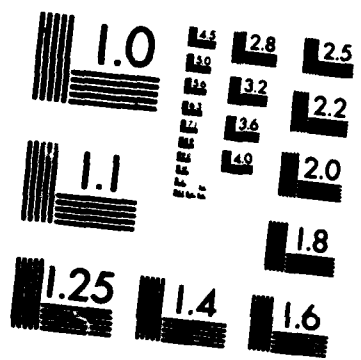
2/2

UNCLASSIFIED

F/G 8/3

NL





MICROCOPY RESOLUTION TEST CHART
NATIONAL BUREAU OF STANDARDS-1963-A

- National Ocean Survey, U.S. Dept. of Commerce, NOAA, California Marine Boundary Program Final Report, 1981.
- National Ocean Survey, U.S. Dept. of Commerce, NOAA, Tide Tables 1976, West Coast of North and South America, 1975.
- Parke, M. E. and Henderschott, M. C., "M2, S2, K1 Models of the Global Ocean Tide on an Elastic Earth," Marine Geodesy, v. 3, pp. 379-408, 1980.
- Schureman, P., Manual of Harmonic Analysis and Prediction of Tides, U.S. Dept. of Commerce, Coast and Geodetic Survey, S.P.98, 1940.
- Scott, D. A., AMBAG Oceanographic Survey, Oceanographic Services, Inc. #168-2, 1973.
- Skogsberg, T., "Hydrography of Monterey Bay, California - Thermal Conditions, 1929-1933," Transactions of the American Philosophical Society, v. 29, pp. 1-152, 1936.
- Spaulding, M. L. and Beauchamp, C. H., "Modeling Tidal Circulation in Coastal Seas," ASCE Journal of Hydraulic Engineering, v. 109, pp. 116-131, January, 1983.
- Tracor, Inc., Estuarine Modeling: An Assessment, U.S. Environmental Protection Agency, Water Pollution Control Research Series 16070 DZV, 1971.

INITIAL DISTRIBUTION LIST

		No. Copies
1.	Defense Technical Information Center Cameron Station Alexandria, VA 22314	2
2.	Library, Code 0142 Naval Postgraduate School Monterey, CA 93943	2
3.	Chairman (Code 63Hr) Department of Oceanography Naval Postgraduate School Monterey, CA 93943	1
4.	Chairman (Code 63Rd) Department of Meteorology Naval Postgraduate School Monterey, CA 93943	1
5.	Dr. William Hart (Code 8100) Naval Oceanographic Office NSTL Station Bay St. Louis, MS 39522	1
6.	Dr. Edward B. Thornton (Code 68Tm) Department of Oceanography Naval Postgraduate School Monterey, CA 93943	2
7.	Christine W. Schomaker, LT, NOAA NOAA, NGDC E/GC3 325 Broadway Boulder, CO 80303	1
8.	Director Naval Oceanography Division Naval Observatory 34th and Massachusetts Avenue NW Washington, D.C. 20390	1
9.	Commander Naval Oceanography Command NSTL Station Bay St. Louis, MS 39522	1
10.	Commanding Officer Naval Oceanographic Office NSTL Station Bay St. Louis, MS 39522	1
11.	Commanding Officer Fleet Numerical Oceanography Center Monterey, CA 93943	1
12.	Commanding Officer Naval Ocean Research and Development Activity NSTL Station Bay St. Louis, MS 39522	1

13. Commanding Officer
Naval Environmental Prediction Research Facility
Monterey, CA 93943 1
14. Chairman, Oceanography Department 1
U. S. Naval Academy
Annapolis, MD 21402
15. Chief of Naval Research 1
800 N. Quincy Street
Arlington, VA 22217
16. Office of Naval Research (Code 420) 1
Naval Ocean Research and Development Activity
800 N. Quincy Street
Arlington, VA 22217
17. Scientific Liaison Office 1
Office of Naval Research
Scripps Institution of Oceanography
La Jolla, CA 92037
18. Library 1
Scripps Institution of Oceanography
P. O. Box 2367
La Jolla, CA 92037
19. Library 1
Department of Oceanography
University of Washington
Seattle, WA 98105
20. Library 1
CICESE
P. O. Box 4803
San Ysidro, CA 92073
21. Library 1
School of Oceanography
Oregon State University
Corvallis, OR 97331
22. Commander 1
Oceanographic Systems Pacific
Box 1390
Pearl Harbor, HI 96860
23. Director, Charting and Geodetic Services (N/CG) 1
National Oceanic and Atmospheric Administration
Rockville, MD 20852
24. Chief, Program Planning, Liaison, 1
and Training (NC2)
National Oceanic and Atmospheric Administration
Rockville, MD 20852
25. Chief, Nautical Charting Division (N/CG2) 1
National Oceanic and Atmospheric Administration
Rockville, MD 20852
26. Chief, Hydrographic Surveys Branch (N/CG24) 1
National Oceanic and Atmospheric Administration
Rockville, MD 20852
27. Director, Pacific Marine Center (N/MOP) 1
National Ocean Service, NOAA
1801 Fairview Avenue East
Seattle, WA 98102

28. Director, Atlantic Marine Center (N/MOA) 1
National Ocean Service, NOAA
439 W. York Street
Norfolk, VA 23510
29. IHO/FIG International Advisory Board 1
International Hydrographic Bureau
Avenue President J. F. Kennedy
Monte Carlo, Monaco
30. Library 1
Moss Landing Marine Lab
California State Colleges
Sandholdt Road
Moss Landing, CA 95039
31. Dr. Luciano Meiorin 1
600 Bancroft Way
Berkeley, CA 94710
32. Dr. Terry Hendrix 1
SCCWRP Mailcode A-022
Scripps Institution of Oceanography
La Jolla, CA 92093
33. LCDR Gerald B. Mills (Code 68Mi) 1
Department of Oceanography
Naval Postgraduate School
Monterey, CA 93943

END

FILMED

12-83

DTIC